

UiT

THE ARCTIC
UNIVERSITY
OF NORWAY

Department of Geosciences, Faculty of Science and Technology

Cryosphere-controlled methane release throughout the last glacial cycle

Pavel Serov

A dissertation for the degree of Philosophiae Doctor – December 2018

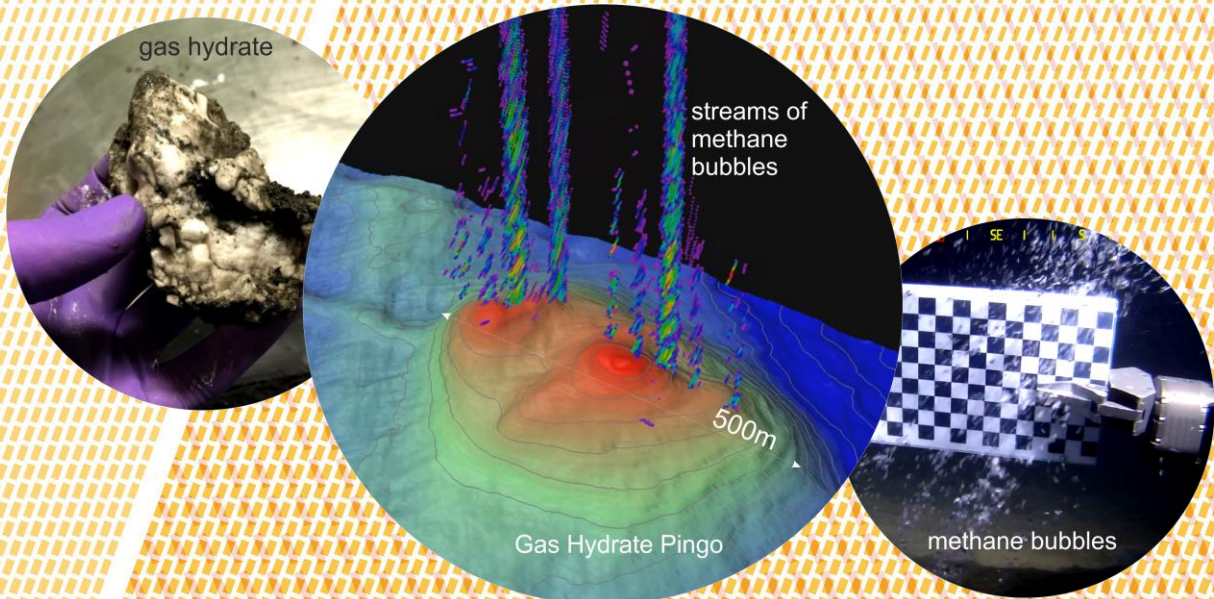


Table of Contents

1	Introduction	3
1.1	Scope	3
1.2	Key concepts and definitions	5
1.3	Evolution of the cryosphere on the Barents Sea shelf and the Kara Sea shelf from the Last Glacial Maximum to the 21 st Century	9
1.4	Three study regions	12
1.4.1	Yamal Shelf (South Kara Sea)	13
1.4.2	Storfjorden Trough (Barents Sea)	15
1.4.3	Bjørnøya Trough (Barents Sea)	16
1.5	Cryosphere-controlled methane capacitors and climate change.....	18
2	Summary of Articles	22
2.1	Article 1	22
2.2	Article 2.....	23
2.3	Article 3.....	24
2.4	Article 4.....	25
2.5	Article 5.....	26
3	Future research	27
	List of figures	28
	Reference.....	29

Preface

The cryosphere of Arctic regions is undergoing rapid change due to century-scale global warming superimposed on millennial-scale natural climatic perturbations that started at the end of the last glacial cycle approximately 20,000 years ago [*Slaymaker and Kelly, 2009*]. The cryosphere refers to areas where low temperatures freeze water and form ice in the ocean (sea ice), on land (glaciers, permafrost, snow cover) and beneath the seabed (offshore permafrost) [*Harris and Murton, 2005*]. These areas may modulate release of greenhouse gases, such as methane and CO₂ into the atmosphere, both from the ocean through a barrier effect of sea ice, and also from land through a sealing effect of permafrost, glaciers and associated gas hydrates. Today's cryosphere shows rapid degradations in various regions of the Arctic, which may act as a climate change amplifier if outgassing of greenhouse gases from formerly stable gas hydrates and biogenic and thermogenic sources reaches the atmosphere [*Callaghan et al., 2011*]. While gas hydrates are widely distributed within cryosphere, they are only stable under low temperature and high pressure conditions [*Ginsburg, 1998*]. Gas hydrate of natural gas is a crystalline water-based structure physically resembling ice and incorporating large concentrations of hydrocarbon gases (predominantly methane; 1 cm³ of methane hydrate contains 150 cm³ of methane) [*Sloan, 2008*]. With this in mind, the doctoral thesis focuses on gas hydrate dynamics in response to the degradation of the cryosphere across the Barents Sea and South Kara Sea continental shelves throughout the last 35,000 years. This doctoral thesis was undertaken at the Department of Geoscience, UiT – The Arctic University of Norway, Tromsø, from January 2015 to December 2018. The research was part of CAGE – Centre for Arctic Gas Hydrate, Environment and Climate funded by the Norwegian research council (grant 223259). CAGE and UiT provided full technical support in acquiring most of the data used in this thesis. Additionally, unique geological, geophysical and geochemical data from the South Kara Sea came from The All-Russian Research Institute of Geology and Mineral Resources of the World Ocean “VNIIOkeangelogia named after I.S. Gramberg”.

During the four years of my doctoral education I participated in 10 research cruises onboard *RV Helmer Hanssen* (nine cruises, 2015-2018) and *RV Kronprins Haakon* (one cruise, 2018) to the northwestern and central Barents Sea for geological and water column sampling and collection of geophysical data (2D high-resolution seismic, P-cable 3D seismic, single- and multibeam echosounder). Participation in these cruises enabled both the collection of necessary multidisciplinary datasets that were used in this doctoral thesis and also the broadening of my understanding of subseafloor gas hydrate and fluid flow systems, the nature of seabed methane release, and the fate of methane in the water column. The collection of empirical data, which was later supported by advanced numerical modeling are deemed fundamental for the five research articles (four published and one manuscript) included in this doctoral thesis. Five evenly important research articles (2 published, 3 submitted) are not included in this thesis to keep the thesis focused. The results from this multidisciplinary research attracted attention in both the

media and on seven international research conferences and workshops. Dissemination efforts of our research resulted in a number of publications in online and printed media sources, including ‘The Washington Post’ and ‘Nauka’ (in Russian).

This doctoral thesis is composed of an introduction and five research articles with short annotations revealing natural environmental changes controlling extensive seabed methane release across the Arctic Ocean Continental margins during the last ~35000 years.



RV Helmer Hanssen off Kvitøya Island (Arctic Ocean; 80.3° N, 31.8° E). Photo by Bjørn Runar Olsen

Supervisors

Prof. Karin Andreasson

CAGE – Centre for Arctic Gas Hydrate, Environment and Climate,
Department of Geosciences,
UiT – the Arctic University of Norway, Tromsø, Norway

Prof. Jürgen Mienert

CAGE – Centre for Arctic Gas Hydrate, Environment and Climate,
Department of Geosciences,
UiT – the Arctic University of Norway, Tromsø, Norway

Prof. JoLynn Carroll

Akvaplan-niva, FRAM – Hight North Research Centre
for Climate and the Environment, Tromsø, Norway
Department of Geosciences,
UiT – the Arctic University of Norway, Tromsø, Norway

Acknowledgements

First of all, I would like to thank my academic advisors, who made it possible for me to start and complete the PhD program. I was truly lucky to work with three excellent advisors without whom my education would not be as exciting and diverse as it was, or would not be possible at all. I would like to express my deep gratitude to Prof. Jürgen Mienert who supervised me from the first day of the PhD training and until the very last hour before this thesis was submitted. His unique way of thinking, creativity and incredibly deep understanding of nature guided me through my work. Prof. Jürgen Mienert believed in me even when I could not find reasons to believe in myself. Working with him was a great adventure that I will remember and be proud of. I would also thank Prof. Karin Andreassen, who accepted a challenge becoming my main supervisor at the last and the most critical year of the PhD project. Her energy and enthusiasm in research always admired me, while her solicitude and support helped me completing the last and the most difficult steps towards finishing this dissertation. Also, my research and education would not be possible without Prof. JoLynn Carroll who started this PhD project and guided my first steps in academia. She showed me a beauty of multidisciplinary approach in science, which I tried to implement throughout my work. These people made my development as a scientist possible.

I am grateful to Prof. Giuliana Panieri, who organized and led my first CAGE cruise onboard RV *Helmer Hanssen*, which became the most exciting research cruise I have ever had. I would also like to thank Prof. Stefan Bünz whose expertise helped me at different stage of this PhD project and at planning the future research.

I would like to thank crew of RV *Helmer Hanssen* and research engineers Steinar Iversen and Bjørn Runar Olsen who helped us collecting truly unique data. I will always remember RV *Helmer Hanssen* where I spent more than 100 days, where discoveries were made, and where new friendships started.

My PhD in Tromsø would not be possible without knowledge, experience and support of Dr. Boris Vanshtein and Prof. Georgy Cherkashov with whom I worked for 7 years. Dr. Boris Vanshtein took me to my first research cruise in the Arctic Ocean when I was 17 years old, after which I never doubted becoming a marine geologist.

I would like to thank my colleagues who helped me developing scientific articles – Alexey Portnov, Sunil Vadakkepuliambatta, Henry Patton, Alun Hubbard, Calvin Shackleton and Anna Silyakova. I very much appreciate our large group of friends coming from all over the world to Northern Norway to work, explore the nature, ski, climb mountains and enjoy life: Alexey Pavlov, Alexey Portnov, Anna, Dasha, Calvin, Mariana, Giacomo, Kate, Carly, Arunima, Friederike, Emmelie, Sunny, Warren, Henry. I owe an immeasurable gratitude to my family and friends from Russia who always supported me despite my work did not allow me spending as much time with them as they deserve.

Yet, my biggest acknowledgement goes to my partner, friend, colleague, ski companion and everlasting motivator – Malin Waage, who always inspires, supports, and loves.

List of Articles

1. Pavel Serov, Alexey Portnov, Jürgen Mienert, Petr Semenov, Polina Ilatovskaya (2015). **Methane release from pingo-like features across the South Kara Sea shelf, an area of thawing offshore permafrost.** *Journal of Geophysical Research: Earth Surface*. DOI: 10.1002/2015JF003467
2. Pavel Serov, Sunil Vadakkepuliambatta, Jürgen Mienert, Henry Patton, Alexey Portnov, Anna Silyakova, Giuliana Panieri, Michael L. Carroll, JoLynn Carroll, Karin Andreassen, Alun Hubbard (2017). **Postglacial response of Arctic Ocean gas hydrates to climatic amelioration.** *Proceedings of the National Academy of Science of the United States of America (PNAS)*. DOI: 10.1073/pnas.1619288114
3. Karin Andreassen, Alun Hubbard, Monica Winsborrow, Henry Patton, Sunil Vadakkepuliambatta, Andreia Plaza-Faverola, Eythor Gudlaugsson, Pavel Serov, Alexey Deryabin, Rune Mattingsdal, Jürgen Mienert, Stefan Bünz (2017). **Massive blow-out crater formed by hydrate-controlled methane expulsion from the Arctic seafloor.** *Science*. DOI: 10.1126/science.aal4500
4. Wei-Li Hong, Marta E. Torres, JoLynn Carroll, Antoine Crémière, Giuliana Panieri, and Pavel Serov (2017). **Seepage from an arctic shallow marine gas hydrate reservoir is insensitive to momentary ocean warming.** *Nature Communications*. DOI: 10.1038/ncomms15745
5. Pavel Serov, Henry Patton, Malin Waage, Calvin Shackleton, Jürgen Mienert, Karin Andreassen (manuscript) **Subglacial denudation of gas hydrate bearing sediments on an Arctic Ocean continental margin.**

1 Introduction

1.1 Scope

This doctoral thesis focuses on gas hydrate dynamics in response to the evolution of the cryosphere across the Barents Sea and South Kara Sea continental shelves throughout the last ~35,000 years until the 21st century. Within this time, our study sites, an area of relic subsea permafrost in the South Kara Sea, and a previously ice-sheet dominated region of the Barents Sea experienced significant climatic amelioration. It led to the ice-sheet retreat from the Barents Sea continental shelf and flooding of Arctic coast, e.g. Siberian coast bearing permafrost. The removal of the ice-sheet load from the Barents Sea shelf and flooding of permafrost on the South Kara Sea coast with water ~ 15 C° warmer than air triggered a destabilization of pressure and/or temperature sensitive gas hydrate and permafrost, and subsequently promoted the release of methane – this is a process that has far reaching consequences until today. There are several aspects of considerable interest relating to the research of cryosphere – controlled methane release:

1. **Scientific aspect.** While it is evident that terrestrial permafrost contains enormous amounts of carbon stored as organic matter, free gas and gas hydrates, the fate of relic subsea permafrost and its role in modulating seabed methane release across the various Arctic regions remains unclear. In light of recent discoveries of methane-related blow-out craters in thawing terrestrial permafrost on Yamal Peninsula close to the Kara Sea [*Moskvitch*, 2014], the continental shelf areas bearing its natural continuation might likewise experience abrupt release of methane caused by ocean warming and/or pressure changes [*Portnov et al.*, 2018]. Thus, observations of fluid/gas release within and from the seabed are important for reconstructing postglacial permafrost dynamics and associated methane release across the underexplored South Kara Sea shelf.

In contrast, seabed expressions of past fluid release (pockmarks, craters, mounds, etc.) across the northwestern Barents Sea are better known due to hydrocarbon exploration in these regions. Despite common understanding that they result from vertical migration and seabed discharge of free gas, the mechanisms that produced the gas remains under discussion, since many of the pockmarks observed inactive today. The combination of an ice-sheet evolution model with a gas hydrate model yields new insights on whether deglaciation caused wide spread gas hydrate dissociation and methane release resulting in abundant fluid escape features.

2. **Climate change aspect.** 21st century and future gradual ocean warming and short-term seasonal temperature changes may force dissociation of gas hydrates within a narrow (< ~10 m) water depth interval, contributing some amounts of greenhouse gas methane to the atmosphere, yet less than previously thought (~6 TG CH₄ yr⁻¹ equal to ~1% of total annual flux from all

sources) [Ruppel and Kessler, 2017]. However, rapid depressurization due to Last Glacial Maximum ice-sheets retreat combined with ocean warming is a potentially stronger mechanism for gas hydrate decomposition on a longer time scale. This could cause release of gas hydrate bound methane at quantities and rates fundamentally different from what is observed today. Given that ice core carbon isotope records cannot distinguish gas hydrate methane from wetland methane (both are $<60\text{‰}$ $\delta^{13}\text{C}$ [Chappellaz *et al.*, 2013]) and δD records only indicate marine source of methane regardless whether it is related to hydrates or not [Sowers, 2006], the question about postglacial gas hydrate methane contribution to atmospheric budget remains open.

3. **Geotechnical aspect.** Decomposition of gas hydrates and thawing of permafrost may shape seafloor and change geotechnical properties of the sediments [Nelson *et al.*, 2001; Sultan *et al.*, 2004]. With a growing number of planned seabed constructions in polar regions (e.g. fiber cables, wind mills) it has become even more important to understand potential consequences of phase changes from ice and hydrate to water and gas within pore space of sediments. Studying seabed imprints of past gas hydrate decomposition and permafrost thaw may therefore yield insights into the extent and magnitude of seabed and subseabed deformations in areas of importance for seabed developments in the 21st century and beyond.

4. **Geohazard aspect.** Since 1 cm³ of gas hydrates contains ~150 cm³ of methane gas, the decomposition of gas hydrates in sediments can cause a rapid volume increase leading to gas accumulations with pressures significantly exceeding hydrostatic pressure. It is critical to identify the likely locations for these gas accumulations in order to reduce the risk for blow-outs during drilling operations. Moreover, over-pressured gas in pore spaces of sediments may compensate for part of the lithostatic stress and decrease strain of sediments leading to submarine mass movements.

5. **Biological aspect.** Seabed methane seeps are key energy sources for chemosynthesis based biological communities in deep water regions devoid of sun light [Levin *et al.*, 2016]. Recent studies of arctic cold seeps showed appreciable increases in the abundance and diversity of infaunal and megafaunal species compared to surrounding areas without seeps [Åström *et al.*, 2018]. In deep-water regions of the continental margins, depletion of conventional food sources may urge conventional heterotrophs to capitalize on the rich biomass of chemosynthesis based ecosystems. Thus, the occurrence of wide-spread seeps across the Barents Sea shelf can play a major role in benthic biological community distributions.

1.2 Key concepts and definitions

Arctic continental margins contain large amount of hydrocarbons [Gautier *et al.*, 2009] and organic matter [Bröder *et al.*, 2018] genuinely fueling seepage of thermogenic and biogenic gas [Ruppel and Kessler, 2017]. Thermogenic hydrocarbons (e.g. **thermogenic methane**) form due to thermal cracking of organic molecules (kerogen) at a temperature of > 60 °C and depth of > 1.5 km. In contrast, **biogenic methane** is a result of organic matter decomposition through metabolic activity of methanogenic microbial communities in shallower subsurfaces (<1 km) [Inagaki *et al.*, 2006]. Since it is not related to substantial burial and high temperatures, biogenic methane generation implies a comparatively rapid turnover of organic matter. Reported ages of biogenic methane are often <1000 years, while the youngest thermogenic hydrocarbon source rocks are of Neogene Age (> 2.6 million years old).

Regardless of its origin, methane may migrate through cracks and effective porosity in lithified rocks or unconsolidated sediments as free gas or in dissolved phase. Diffusion is deemed comparatively inefficient in transporting methane over large areas and forming any substantial accumulations [Judd and Hovland, 2009]. Advective methane flow driven by buoyance force and pressure gradients tends to reach higher hypsometric levels and may eventually expel at the seafloor. Noteworthy, across continental margins, the ascending flux of dissolved methane experiences sufficient reduction due to anaerobic oxidation in bottom sediments [Boetius *et al.*, 2000]. **Anaerobic oxidation of methane (AOM)** is a process of methane oxidation with different electron acceptors (most commonly sulfate) in anoxic marine or freshwater conditions. Methane oxidation is coupled with sulfate reduction through a consortium of methanotrophic archaea and sulfate-reducing bacteria [Boetius *et al.*, 2000]. Their symbiosis causes specific biogeochemical interface called **sulfate-methane transition zone** where sediment pore water sulfate infiltrating from sweater and methane migrating from deeper sediments experience coupled reduction. 80-90 % of the upward diffusive methane flux (400 Tg CH₄ y⁻¹ estimated globally) oxidizes anaerobically [Reeburgh, 2007].

Beyond this strong microbiological methane filter, geological structures impermeable for fluids constitute physical barriers retaining dissolved and gaseous methane. Similar to geological seals, subsea permafrost and gas hydrates have the potential to limit vertical methane flux [Archer, 2015; Dickens *et al.*, 1997] with one fundamental difference: they are particularly sensitive to environmental conditions such as pressure and temperature and may rapidly form or degrade .

Subsea permafrost – submerged grounds/sediments that remain below freezing point for two or more consecutive years. Subsea permafrost may form on the continental shelves of polar regions during episodes of sea-level lowstands and low-temperature exposure, or in subsea conditions in response to negative mean annual bottom temperatures. Frozen deposits are less permeable [Yakushev and Chuvilin,

2000] or impermeable [Shakhova *et al.*, 2010] for fluids acting as a seal and isolate organic matter within its frozen framework. Thawing of permafrost uncaps the fluid flow and liberates organic matter supporting methanogenesis. Low temperatures within subsea permafrost may sustain gas hydrates in low-pressure conditions of shallow shelves and onshore.

Gas hydrates of natural gas – crystalline solids consisting of methane and its heavier homologs (e.g. ethane, propane) trapped in a lattice of hydrogen-bonded molecules of water. Under stable – low temperature, high pressure – conditions, gas hydrates act as an efficient methane sink (1 cm³ of methane hydrate contains ~150 cm³ of gas). If hydrate-bearing sediments abandon the gas hydrate stability envelop, hydrates dissociate releasing free gas. Gas hydrates are widely distributed on continental slopes, overdeepened shelves and in subsea and terrestrial permafrost (intra-permafrost gas hydrates). Grounded ice-sheets feature another strong control on gas hydrate distribution. Loading of ice provides high pressure which along with low basal temperatures generates a **subglacial gas hydrate stability zone** [Portnov *et al.*, 2016; Wadham *et al.*, 2012]. Upon ice-sheet retreat, subglacial gas hydrates may be outside the gas hydrate stability zone (GHSZ) and dissociate releasing methane from the seabed [Long *et al.*, 1998].

The area of the seafloor with enhanced concentrations of methane surrounding a vent of methane bubbles is called a **methane seep**. At seep sites, methane and hydrogen sulfide – a product of AOM – is an energy source supporting specific seafloor ecosystems [Ruff *et al.*, 2015]. Another byproduct of AOM – bicarbonate may facilitate precipitation of methane-derived authigenic carbonates. Paragenesis of authigenic carbonates and chemosymbiotic fauna (Figure 1) is a strong indicator of present or paleo methane rich environments.

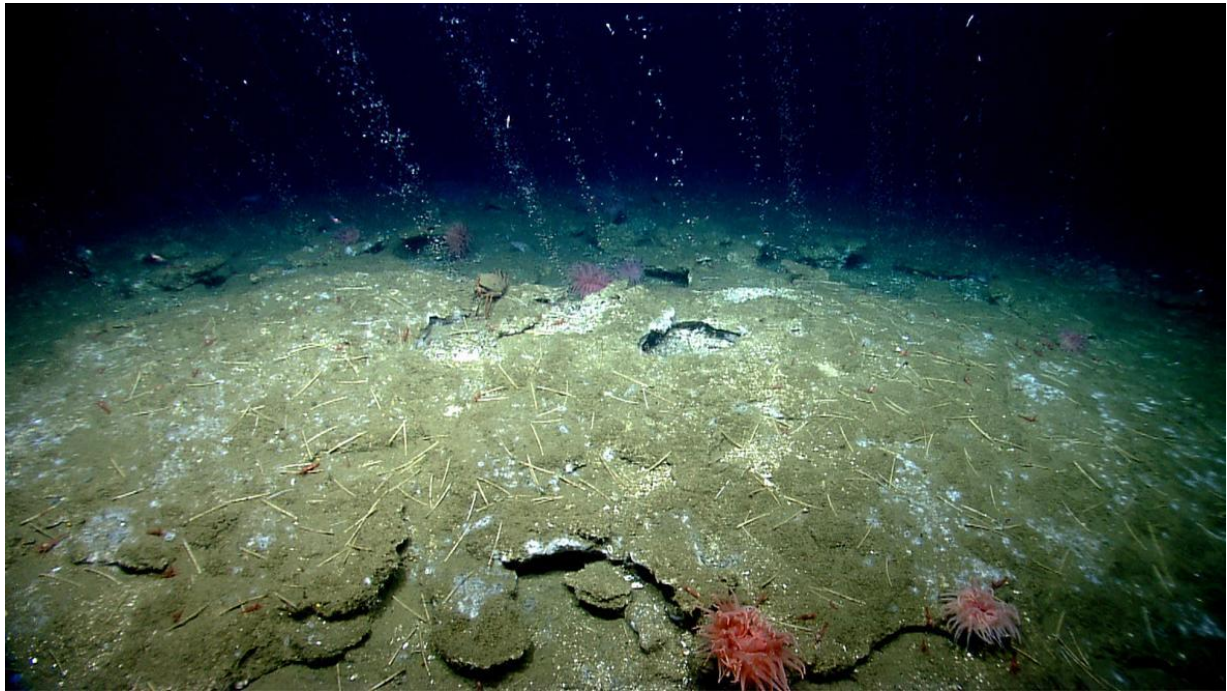


Figure 1 – Release of methane gas and surrounding pavements of authigenic carbonates offshore Virginia, Atlantic Ocean. Image by NOAA Okeanos Explorer program, 2013 Northeast U.S. Expedition. Public domain.

Fluid flow and gas hydrate dynamics cause origination of specific seafloor structures, such as pockmarks, mud volcanoes, gas hydrate pingos, craters, etc. The latter is suggested to be a manifestation of blow out methane discharge tracing collapse of Arctic gas hydrate and permafrost systems [Kizyakov *et al.*, 2017; Long *et al.*, 1998; Moskvitch, 2014].

Gas hydrate pingos – seafloor mounds composed of deposits containing substantial quantities of gas hydrates and capping a strong methane inflow (Figure 2). Seep related authigenic carbonates and permafrost may contribute to solid content of gas hydrate pingos (GHPs). GHPs are suggested to originate due to one or combination of following: frost heaving, gas hydrate heaving, volume expansion when hydrates decompose and extrusion by overpressured gas accumulations [Koch *et al.*, 2015; Paull *et al.*, 2007; Serié *et al.*, 2012].

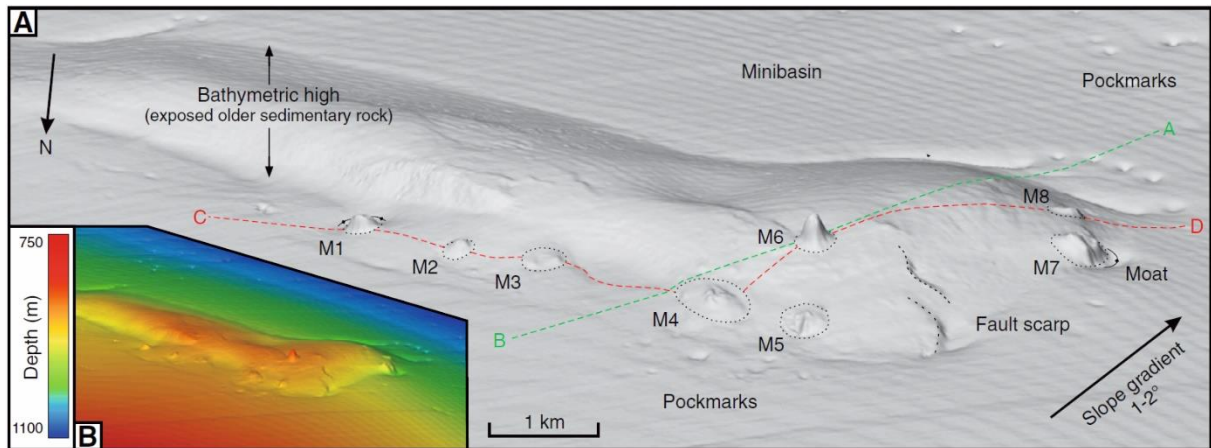


Figure 2 – Gas hydrate pingos (M1 – M8) on shaded relief map (A) and bathymetric map (B) in the Kwanza Basin, offshore Angola [Serié *et al.*, 2012].

Seafloor craters – spherical depressions cut in the seafloor with steep walls (up to 45°) and diameter typically exceeding 500 m. Compared to pockmarks, craters are larger, deeper and may develop in lithified rocks [Long *et al.*, 1998]. The natural craters are hypothesized to originate due to blow outs of fluids analogous to the features formed due to human-caused blow-out accidents during drilling operations (Figure 3) [Leifer and Judd, 2015].

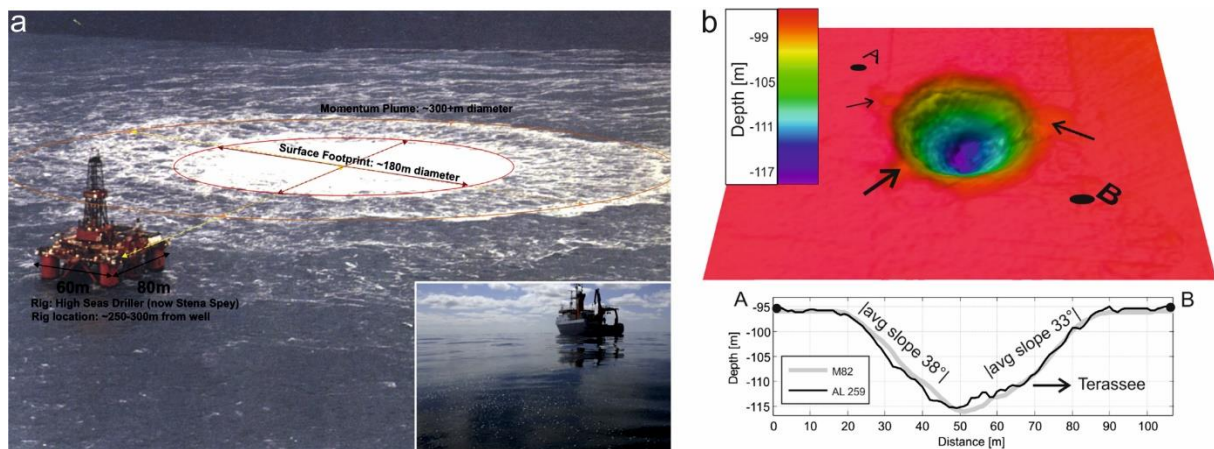


Figure 3 - Blowout at 22/4b well in the North Sea, November 1990 (modified after Leifer and Judd [2015] and Schneider von Deimling *et al.* [2015]). a - surface expression of a gas plume. Insert shows gas bubbles observed on the sea surface at 22/4b site during a research cruise in 2005 [Leifer and Judd, 2015]; b – gridded multibeam bathymetry data and a topographic profile showing 20 m deep crater formed at the site [Schneider von Deimling *et al.*, 2015].

1.3 Evolution of the cryosphere on the Barents Sea shelf and the Kara Sea shelf from the Last Glacial Maximum to the 21st Century

The Last Glacial Maximum (LGM) is the most recent period in Earth history when global ice-sheet volume reached its maximum values and associated global sea-level its minimum with ~120 m fall. Starting at 33,000 years BP a combined effect of decreases in northern summer insolation, atmospheric CO₂, and sea surface temperature in tropical regions of the Pacific Ocean provoked growth of the ice-sheets to their maximum configurations [*Mix et al.*, 2001]. The maximum extent of ice-sheets across the globe occurred between 26,500 and 19,000 years BP sustained by comparatively stable climate for ~7,500 years [*Clark et al.*, 2009]. ~19,000 years BP orbitally induced increase in insolation triggered a suite of feedbacks (greenhouse gas, sea-level, ice albedo, and wind feedbacks) triggering global nearly synchronous deglaciation [*Alley and Clark*, 1999].

During the LGM the Barents Sea and western parts of the Kara Sea were covered by a marine-based Barents Sea Ice-sheet, which was a part of the Eurasian ice-sheet complex [*Jakobsson et al.*, 2014; *Patton et al.*, 2016]. At its maximum configuration the ice-sheet reached the shelf break on the western and northern margins of the Barents Sea, but it was terminated at and did not reach across the South Kara Sea. Towards the south it joined the terrestrial-based Fennoscandian Ice-sheet (Figure 4).

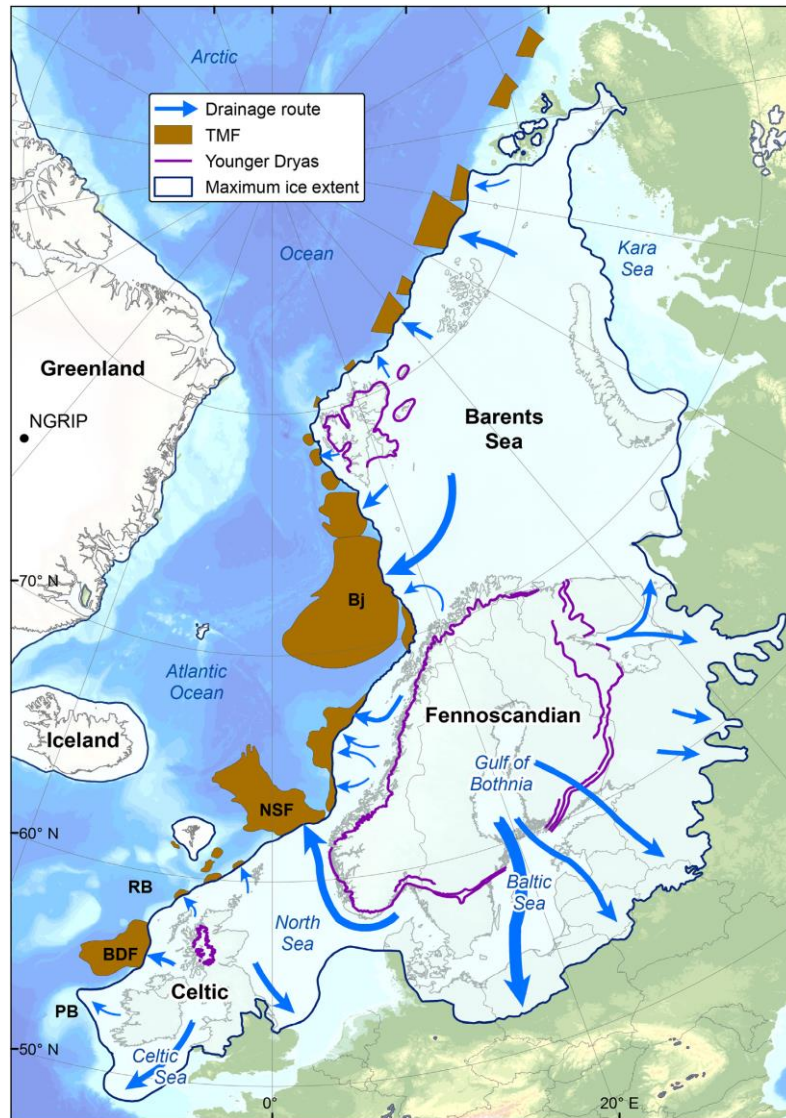


Figure 4 – Maximum ice-sheet extent of the Barents Sea and Fennoscandian Ice-sheets and their major drainage pathways [Patton *et al.*, 2017].

The Barents Sea Ice-sheet at its LGM configuration reached >2 km thickness and substantially loaded the underlying lithosphere [Patton *et al.*, 2016]. Subsequent decay of the ice-sheet caused isostatic rebound [Siebert *et al.*, 2001] locally outpacing sea-level change [Wallmann *et al.*, 2018]. This may have an important implication for the stability of shallow submarine gas hydrates as well as deep hydrocarbon gas accumulations. Numerical modeling of isostatic adjustments of the Barents Sea shelf coupled with sea level curves reveal substantial shallowing of vast areas of the Barents Sea shelf (Figure 5) [Patton *et al.*, 2016]. A significant decrease of water depth (pressure) may cause a thinning of GHSZ, and destabilization of gas hydrates at its base. Noteworthy, the central part of the Barents Sea experienced a decrease in water depth from > 400 m to < 300 m that caused a complete disappearance of gas hydrate reservoirs accompanied by extensive seabed methane release.

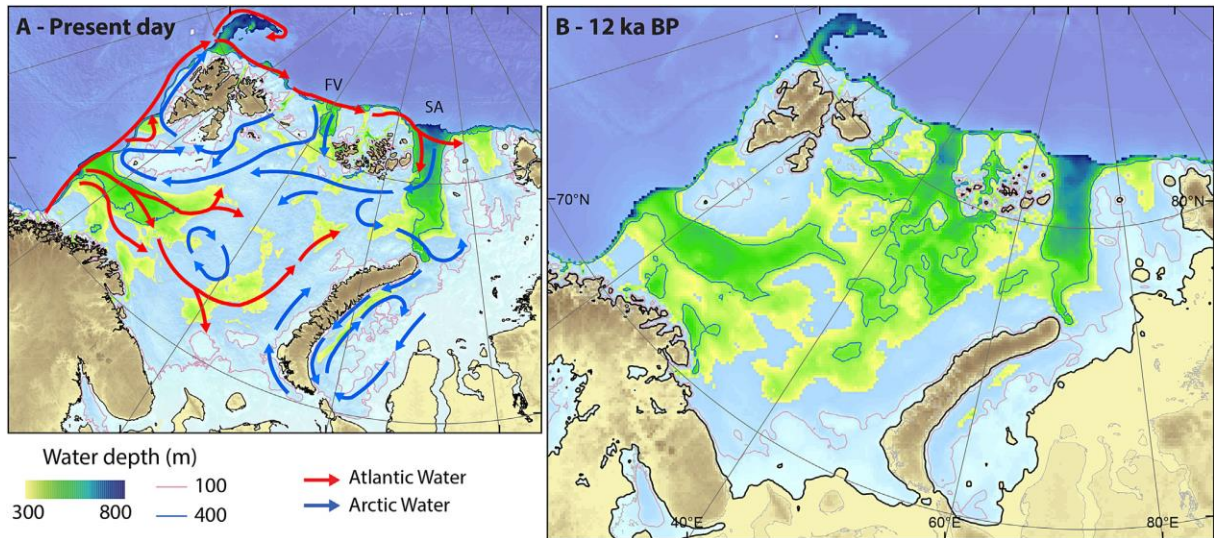


Figure 5 – seabed topography change due to isostatic rebound of the Barents Sea shelf [Patton *et al.*, 2017].

During the LGM, the South Kara Sea was located on a margin of the Barents Sea Ice-sheet with ice thickness < 500 m. Therefore, it only experienced minor isostatic adjustments. The local sea-level here is dominated by global sea-level trends (Figure 6). Due to the LGM sea-level lowstand the Kara Sea coastline was located at the present day ~120 m isobath. Its shelf seas, which now experience <120 m of water depth were exposed to air with a mean annual air temperatures of < -15 °C.

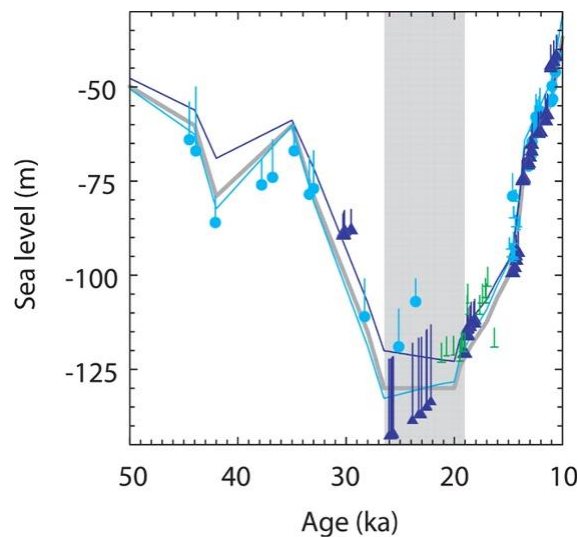


Figure 6 – Global sea-level predictions (lines) and relative sea-level data (dots) for New Guinea (light blue) and Barbados (dark blue). Grey line indicates eustatic sea-level time series [Clark *et al.*, 2009].

1.4 Three study regions

This thesis focuses on four geographical regions demonstrating methane release, which were directly or indirectly affected by the last glaciation. Study areas 1 and 2 (Article 1) are located outside the LGM limits of the Barents Sea Ice-sheet within shallow water (40-80 m water depth) of the Yamal Shelf at the South Kara Sea (Figure 7). During the glaciation, the shallow shelves of the Arctic Ocean, including Yamal Shelf emerged, were subaerial and experienced freezing under mean annual temperatures as low as $-15\text{ }^{\circ}\text{C}$. In contrast, our study sites 3 and 4 (Articles 2-5) were covered by $> 1500\text{ m}$ thick grounded Barents Sea Ice-sheet (Figure 4), which insulated the lithosphere and provided substantial loading. High pressure conditions under the ice-sheet and low temperature permafrost conditions outside it are favorable for increasing gas hydrate stability and methane sequestration. Yet, depending on different phases of the cryosphere development related to thickness and temperature such methane inventories may have experienced non-synchronous dissociation driven by the large-scale natural climatic amelioration that started $\sim 20,000$ years BP.

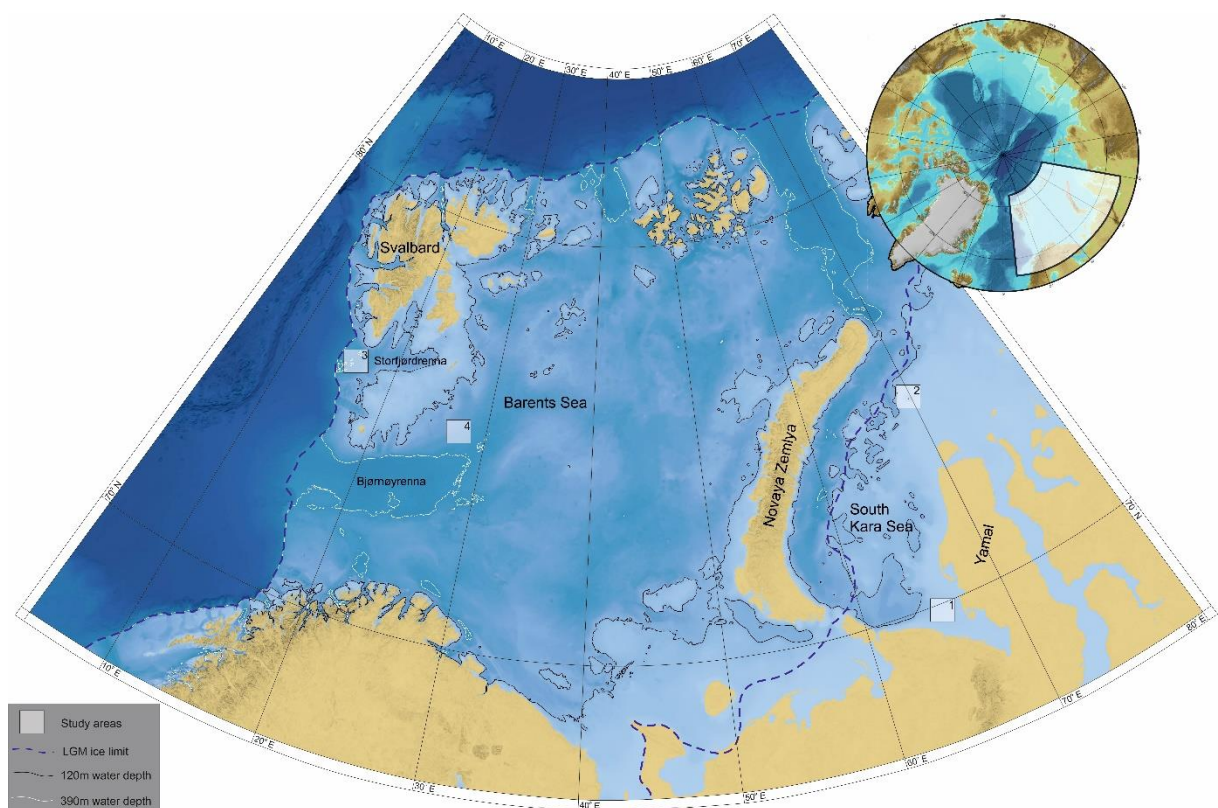


Figure 7 – Location of the study areas in relation to limits of the LGM Barents Sea Ice-sheet, 120m isobath marking the maximum seaward limit of relic subsea permafrost, and 390m isobaths indicating tentative shallow termination of methane hydrate stability zone [Jakobsson *et al.*, 2012].

1.4.1 Yamal Shelf (South Kara Sea)

The shallow (<120 m water depth) shelf offshore Yamal Peninsula is 100 – 120 km wide and does not demonstrate any significant seafloor relief. Considering the low gradients even minor sea-level fluctuations will cause large-scale advances or retreats of the shoreline. Existing eustatic sea level curves reveal that distal parts of shelf that are deeper than 55 m were exposed and thus experienced freezing for minimum ~22,000 years, while shallower areas experienced freezing for as long as ~65,000 years (Figure 8). Ice-sheet modeling and empirical observations suggest insignificant glacio-isostatic movement along the Yamal coastlines indicating minimal deviations from the global sea-level trend (Figure 8).

During periods of shelf exposure, the low mean annual air temperatures provoked growth of up to ~300 m thick permafrost that partly exists until today [Yakushev and Chuvilin, 2000]. Coastal inundation started ~19,000 years BP causing a >10 °C warming of the seafloor initiating thawing of relic permafrost. Current state of relic subsea permafrost in the South Kara Sea is still controversial. Modeling studies by Portnov *et al.* [2014] suggest a range of possible rates of permafrost retreat and propose the most likely scenario of present seaward limit of continuous permafrost at c. 20 m water depth. Notably, the seabed methane release sites concentrate in the region deeper than 20 m water depth (Figure 9). In contrast, mapping of acoustic signatures of permafrost suggest that subsea permafrost extends to 60 m water depth [Rekant and Vasiliev, 2011]. Drilling data reveal occasional subsea permafrost at 0 – 130 m water depths. Contradictions between modeling, direct and indirect empirical observations may point towards a heterogenous state of subsea permafrost in different areas of the Yamal Shelf causing a patchy distribution.

Beneath the South Kara Sea exists a 7-10 km thick Mesozoic and upper Cenozoic sedimentary basin containing source rocks analogous to West Siberian petroleum province [Stupakova, 2011]. Yamal peninsula adjacent to our offshore study sites 1 and 2 hosts 26 gas, gas condensate and oil fields [Grama, 2012]. In these offshore areas conventional seismic data show numerous prospective structures with a potential for gas and gas condensate.

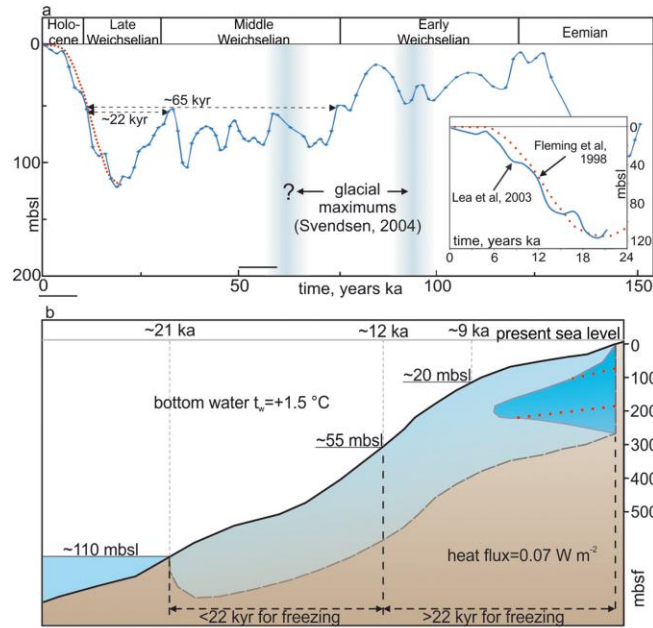


Figure 8 – (a) Eustatic sea level curves defining exposure time of the Yamal Shelf [Fleming *et al.*, 1998; Lea *et al.*, 2003]. (b) Modeled extent of permafrost during the LGM sea level lowstand (light blue) and today (dark blue) [Portnov *et al.*, 2014].

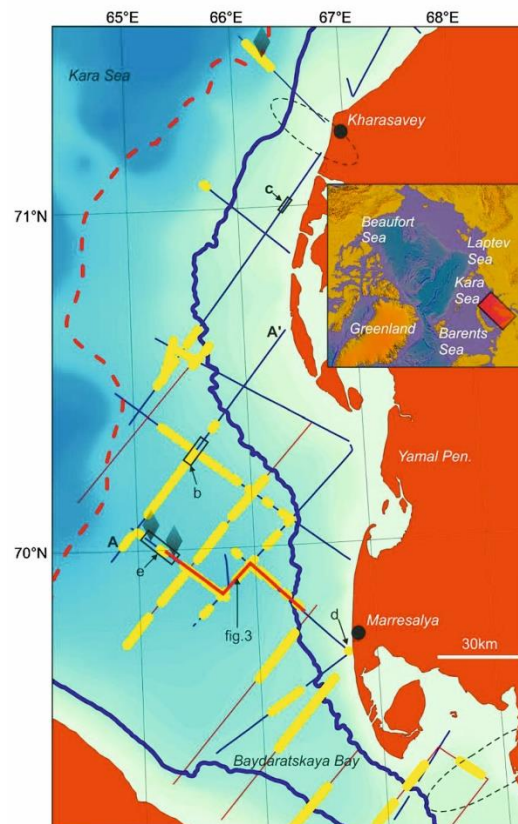


Figure 9 – Hydro-acoustic anomalies on Yamal shelf (yellow lines) concentrating in water depth deeper than 20 m (shown in blue). Black lines show locations of survey lines [Portnov *et al.*, 2013].

1.4.2 Storfjorden Trough (Barents Sea)

Our study site in Storfjorden Trough (Storfjordrenna) shows a specific geological character with a cluster of gas hydrate pingos leaking free gas into the water column (Articles 2, 4, 5). It is located ~50 km southward from Svalbard and ~35 km westward from the shelf break of the Barents Sea. Storfjorden trough is the second largest in the western Barents Sea and was developed by dynamic ice stream draining substantial portions of the Barents Sea Ice-sheet during the last glaciation. Today's seabed of the trough demonstrates a series of grounding zone wedges each reflecting an episode of ice stream standstill during deglaciation. The trough terminates with a large trough mouth fan – a pronounced sediment depocenter on the continental slope. Ice-sheet modeling suggests that our study site was covered by grounded ice up to 2 km in thickness from ~33,000 to ~19,000 years BP [Patton *et al.*, 2017]. After the deglaciation, relaxation of underlying lithosphere resulted in glacioisostatic adjustments that are still ongoing until today [Auriac *et al.*, 2016].

The trough itself shows a thin (< 4 m) veneer of Holocene and postglacial marine muds [Rasmussen *et al.*, 2007] overlying ~100 m thick glacial till. The tills are lying with a distinct angular unconformity (so-called Upper Regional Unconformity - URU) on lithified bedrocks of variable age and origin [Bergh and Grogan, 2003]. Within our ~25 km² study region the glacial unit is remarkably thin and overlies rotated basement blocks of Paleogene age [Lasabuda *et al.*, 2018]. Here, we observe characteristic and wide-spread seismic indications of free gas accumulations. An array of listric faults suggests an extensional tectonic regime that very likely relates to the Hornsund Fault Zone Complex marking a transition zone between continental and oceanic crust along the western Svalbard margin [Anell *et al.*, 2016].

A distinct field of gas hydrate pingos exists on an elongated topographic depression hosting (< ~ 50 m) GHSZ. Along the western Svalbard margin >1200 methane seeps have been mapped close to termination of the GHSZ, yet the majority of them is restricted to bathymetric highs in between glacial troughs [Mau *et al.*, 2017]. Despite the inferred shallow gas hydrate accumulations along the western Svalbard margin, previous sampling attempts (drilling and gravity coring) to recover gas hydrates were unsuccessful. Our study site in Storfjorden trough was the first one with recovered gas hydrates on the shelf surrounding Svalbard.

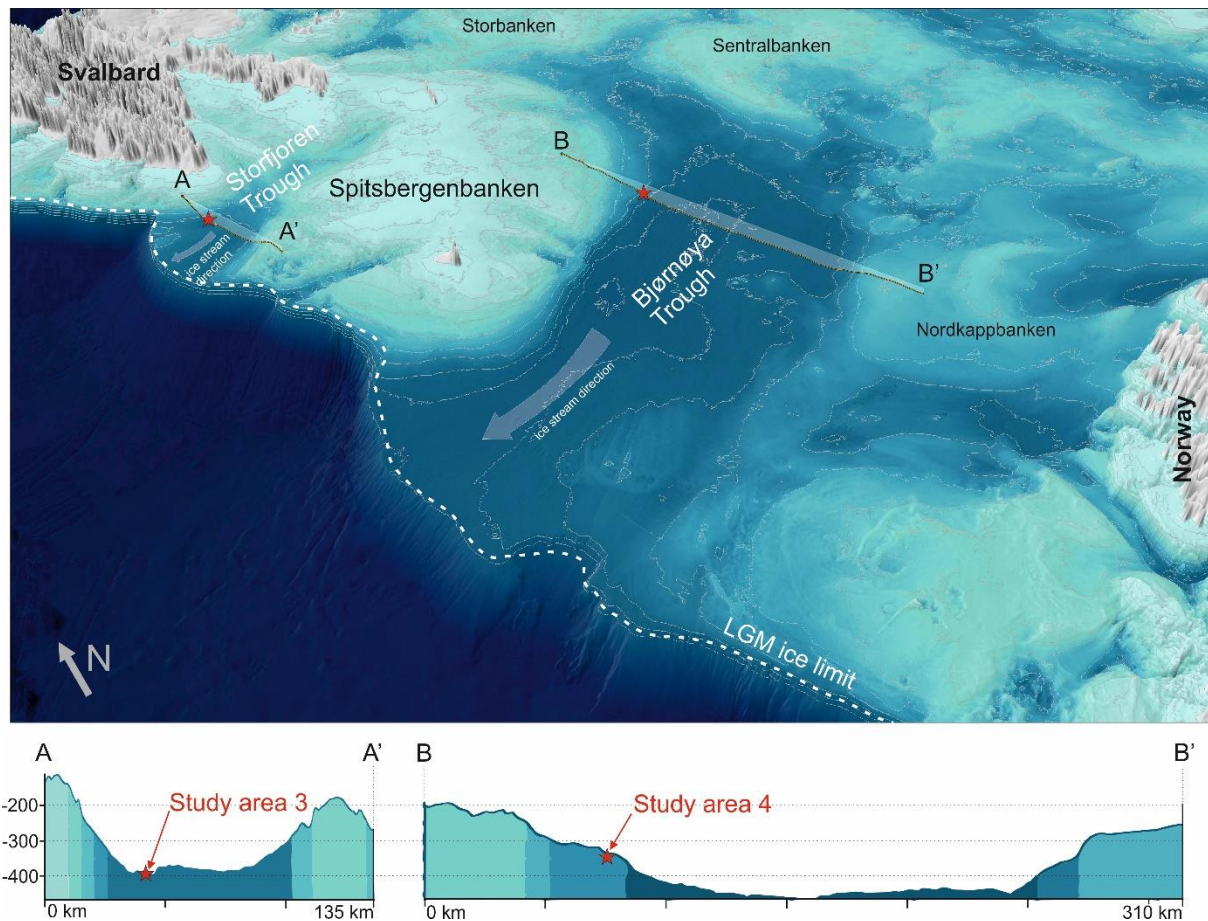


Figure 10 - Seabed topography of the western Barents Sea margin with location of study areas 3 in Storfjorden trough and study area 4 in Bjørnøya trough [Jakobsson *et al.*, 2012].

1.4.3 Bjørnøya Trough (Barents Sea)

Study area 4 (Article 3) stretches along a flank of Bjørnøya Trough (Bjørnøyrenna) – the largest glacially eroded trough crosscutting the Barents Sea shelf from east to west (Figure 10). This study region comprises >100 seabed craters that occur 350 km eastward from the shelf break and c. 200 km distance from Bjørnøya (Bear Island). The sediment blanket is thin [Long *et al.*, 1998] and the thickness of Holocene soft sediments varies from 0 - 30 cm at the study site. Moreover, the glacial unit is essentially missing but outcrops of lithified shales/fine-grained sandstones mark the seabed [Long *et al.*, 1998].

The glacial geomorphology of the trough reveals several grounding zone wedges to the west from the study site marking episodes of decreased ice dynamics during the ice stream retreat [Winsborrow *et al.*, 2010]. Our study site does not show elements of mega-scale glacial geomorphology (streamlined landforms, sediment wedges, etc.), yet reveals numerous ice scouring ploughmarks. Ploughmarks

formed by iceberg activity proximal to retreating ice stream front may provide important insights into the age of the craters.

The Barents Sea experienced extensive Cenozoic erosion that removed up to 3 km of sedimentary strata [Laberg *et al.*, 2012]. Within our study area the glacial erosion has reached down to a series of clinoform structures of Middle-Triassic age. It is known from offshore drilling and outcrops on Svalbard that such clinoforms contain topsets of sandstone and bottomsets of organic-rich fine-grained material [Høy and Lundschieen, 2011; Lundschieen *et al.*, 2014]. Seismic surveys indicated offsets of reflectors within bedrocks pointing towards faulting below the craters [Andreassen *et al.*, 2017]. Therefore, within our study area 4 we anticipate that several crucial components exist for a hydrocarbon leakage system: potential organic-rich source rocks coarsening upwards, disrupted by faults supporting fluid advection. Yet, before our investigations in 2014-2016 seabed fluid release has not been studied in detail. Moreover, the quality of 2D seismic data did not allow documenting subseabed fluid flow, which has now been much improved due to our high-resolution P-Cable 3D seismic survey. Long *et al.* [1998] were only able to hypothesize that craters might have formed due to rapid dissociation of gas hydrates and methane release following ice-sheet retreat during the last deglaciation. Though a hypothesis was postulated, a confirmation of fluid flow systems in the area with integrated modeling of the LGM ice-sheet and gas hydrate evolution were still missing.

Our recent comprehensive ice-sheet modeling suggests that the study area in Bjørnøya trough hosted an ice stream up to 2 km thick from at least 30,000 to 16,000 years ago [Patton *et al.*, 2017]. Outcomes of this model including transient ice-sheet thickness, basal thermal regime and isostatic adjustments of underlying lithosphere provide a solid base to develop a coupled gas hydrate evolution model to investigate the history of methane capture and release in the Bjørnøya trough crater field from the LGM to the 21st Century. Considering present bottom water temperatures, the crater field is mostly lying outside of theoretical methane hydrate stability zone [Vadakkepuliyambatta *et al.*, 2017].

Study area 3 and 4 experienced different histories of pressure and temperature perturbations related to the latest glaciation-deglaciation. Study area 3 lies in the outer part of Storfjorden trough which was deglaciated ~5,000 years earlier if compared to study area 4 located in central part of the LGM ice-sheet (Figures 7, 10). The Storfjorden trough bears a nearly complete LGM – Holocene sediment record that are missing in Bjørnøya trough where lithified bedrocks outcrop on the seabed. Today, a pressure-temperature envelop of methane hydrate stability characterizes the gas hydrate pingo region, but it does not exist anymore in the crater field. Clearly, the seabed structures with the study regions 3 and 4 are very different: while gas hydrate bearing pingos of soft muds exist in area 3, craters and mounds of lithified bedrocks without confirmed gas hydrates exist in area 4.

1.5 Cryosphere-controlled methane capacitors and climate change

Remarkable temperature changes (up to 8 °C [Alley, 2000]) during the glacial-interglacial transitions (as indicated by deuterium content of ice) cannot be quantitatively explained by insolation forcing alone [Brook, 2005]. With growing numbers of atmospheric gas records from ice core samples covering the past 650,000 years it became clear that climate and greenhouse gas cycles are related and the latter contribute ~40% to the radiative forcing (Figure 11).

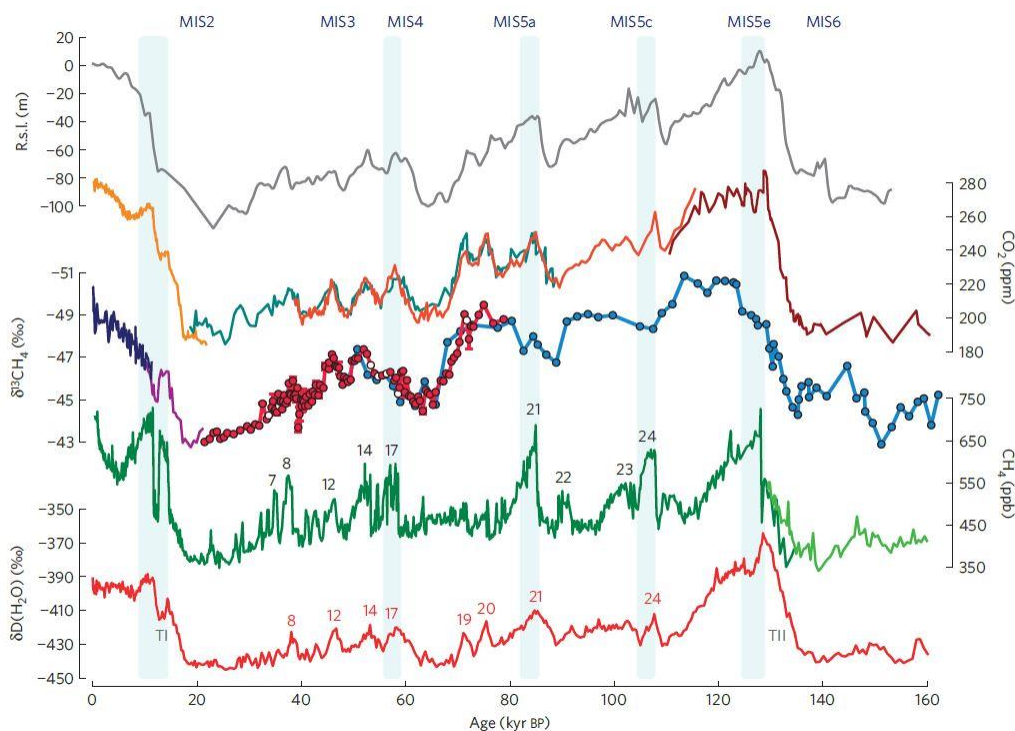


Figure 11 – δD H₂O, methane, $\delta^{13}CH_4$ and carbon dioxide records [Moller *et al.*, 2013]. Ice cores from Vostok, EDML, Talos Dome, Byrd, EPICA Dome C and GISP2 are used for composed curves.

Carbon dioxide and methane have a special relevance to greenhouse gas driven climate warming [Pachauri *et al.*, 2014]. CO₂ is the largest contributor to the radiative effect (its modern atmospheric concentration is ~400 ppm), while CH₄ is the most potent greenhouse gas despite its concentration in the atmosphere is ~220 times less [Stocker, 2014]. Over a 20-year period, one mass unit of CH₄ has 84 times higher impact on the radiative warming than CO₂ and 25 times higher over a century [Stocker, 2014]. In 2017 human-induced warming reached a benchmark value of 1 °C above pre-industrial time (IPCC special report on Global warming of 1.5 °C). Future climate projections reveal a range of global temperature rise scenarios in response to variable CO₂ release rates (Figure 12). Even the scenario with no human-induced radiative forcing after 2055 is predicting a temperate rise throughout the 21st century.

No reduction of net CO₂ radiative forcing will bring us to 1.5 °C warming above pre-industrial time already by 2040 (IPCC special report on Global warming of 1.5 °C). This may have extensive impacts on the temperature-dependent cryosphere and carbon inventories associated to it. Today's climate already forces ice-sheet retreats [Hanna *et al.*, 2008; Rignot and Thomas, 2002], Arctic sea ice decline [Parkinson and Cavalieri, 2008; Sévellec *et al.*, 2017] and permafrost thaw [Sazonova *et al.*, 2004].

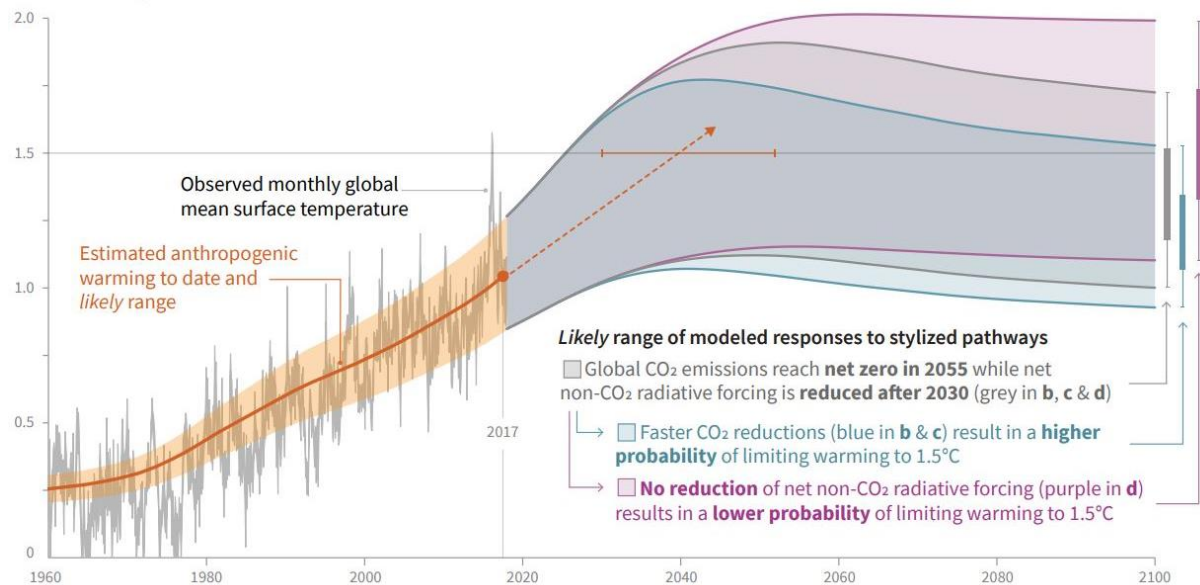


Figure 12 – Observed global temperature changes and modeled future climatic feedback in response to variable anthropogenic CO₂ emission scenarios (IPCC special report on Global warming of 1.5 °C).

Among the subsea CH₄ carbon reservoirs, gas hydrates and permafrost are deemed the most important to the ocean-atmosphere system because of their vast distribution and inconstancy [Ruppel and Kessler, 2017]. Permafrost and gas hydrates are major carbon sinks and storage capacitors for carbon, should the environmental conditions support them. Once temperature and/or pressure becomes insufficient, the capacitors turn into strong emitters of CH₄ carbon. The complex nature of subsea permafrost and gas hydrates that are, on one hand are dependent on, but on the other hand, may modulate the global climate through emissions of CH₄ remains a major discussion point today [James *et al.*, 2016; Ruppel and Kessler, 2017; Shakhova *et al.*, 2015]. In response to a natural warming climate scenario during interglacials, the cryosphere may have controlled intra-permafrost and subglacial gas hydrate reservoirs collapse [Portnov *et al.*, 2014; Portnov *et al.*, 2016]. Despite the fact that interglacial hydrate destabilization events were indeed deciphered in marine sediments [Cremiere *et al.*, 2016; Hill *et al.*, 2006], the contribution of this extensive submarine gas source to the atmosphere remains controversial.

Comparing present terrestrial permafrost and gas hydrate systems with their marine counterparts, the latter ones appear less efficient contributors to atmospheric methane pool due to microbial filter systems within the bottom sediments [Boetius *et al.*, 2000] and the overlying water column [Steinle *et al.*, 2015]. Recent studies suggest that on the Arctic Shelves (90 – 459 m water depth) only 0.07% of all methane entering the water column reaches the atmosphere [Graves *et al.*, 2015; Mau *et al.*, 2017]. Corresponding to these conservative estimates, measurements of methane concentrations above sea-air interface at western Svalbard margin seepage sites claim absence of ocean-atmosphere methane flux, yet one hotspot is reported just north of Svalbard [Myhre *et al.*, 2016; Platt *et al.*, 2018]. Contemporary total flux of methane across the ocean seafloor is 16 – 3,200 Tg CH₄ y⁻¹ [Ruppel and Kessler, 2017], while the total emission of methane from ocean surface to atmosphere is ~0.6 to 10 Tg CH₄ y⁻¹. For comparison, total emissions from natural wetlands vary from ~175 to ~217 Tg CH₄ y⁻¹ [Cranston, 1994; Rhee *et al.*, 2009].

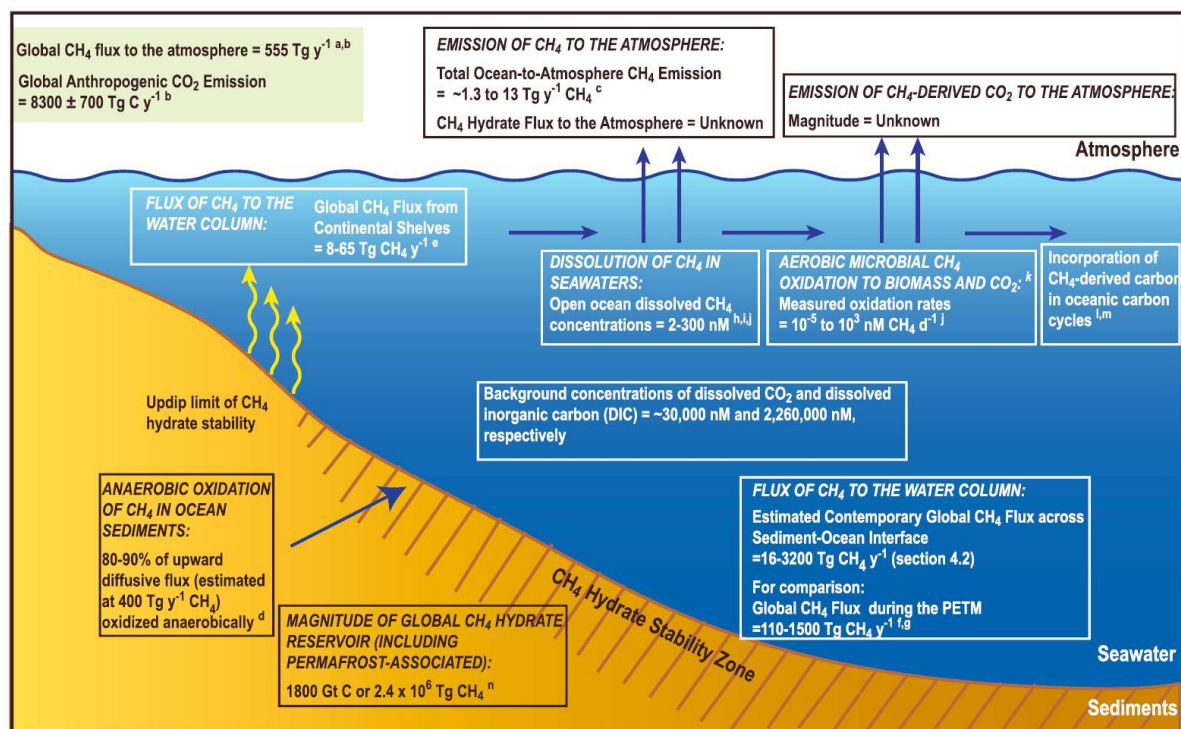


Figure 13 - Sources and sinks of hydrate-bound methane [Ruppel and Kessler, 2017]

Today's CH₄ carbon system is largely described by sinks and sources which are only tentatively quantified (Figure 13) [Ruppel and Kessler, 2017]. Much less is known about past methane inventories modulated by cold or warm climates. During Late Glacial Maximum, the Barents Sea Ice-sheet covered an enormous area of 2.4 x 10⁶ km², including the entire Barents Sea shelf [Patton *et al.*, 2015]. Vast amounts of presently active methane seepage sites were covered by more than 1000 m thick ice-sheet and thus immobilized within the thick subglacial gas hydrate stability zone [Portnov *et al.*, 2016]. A cluster of methane seeps (~500 individual flares within 4 km²) on the western Svalbard margin shows

activity at today's water depth of ~240 m contributing ~438,400,000 g CH₄ y⁻¹ [Sahling *et al.*, 2014]. Assuming the grounded ice-sheet covered this area for at least 5,000 years [Patton *et al.*, 2017] and constant methane flux that can be assumed to be equal to today's flux, up to 2.192 Tg CH₄ might have been subglacially isolated within the area. Estimates of subglacial methanogenesis suggest that 22 to 4680 Gt CH₄ carbon were stored in situ under Northern Hemisphere LGM ice-sheets [Wadham *et al.*, 2008]. Proportion of thermogenic methane involved in subglacial methane cycle is yet to be determined.

Upon ice-sheet collapse rapid and extensive seafloor methane discharge may happen. Proportion of dissolved methane increases as the gas bubbles rise through the water column. The water depth has a primary control on the timing of bubble exposure to solvent and, thus, is a first order measure of ocean methane utilization [Greinert *et al.*, 2006]. Dissolved methane is further subjected to aerobic oxidation [Graves *et al.*, 2015]. However, it is unknown how fast the seawater microbial population grows in response to an increase of methane concentrations. Thus, it is not unlikely, that massive seabed methane release at least for a short time period is not balanced with microbial consumption [Du and Kessler, 2012; Mau *et al.*, 2013]. Growing methane concentrations in surface waters facilitate sea-atmosphere methane flux. However, they may also increase the biological productivity of the surface water causing withdrawal of CO₂ from atmosphere [Pohlman *et al.*, 2017].

Apart from dissolved gas, releases of large quantities of free gas analogous to offshore drilling blowouts may reach the sea-air interface [Leifer and Judd, 2015]. Blowouts are likely to cause upwelling of water with high concentration of dissolved methane that means reduced concentration gradient between the gas bubble and ambient water inhibiting methane dissolution and supporting free gas transport [Leifer *et al.*, 2006]. Blowout events due to abrupt postglacial methane release has been suggested for the Barents Sea shelf [Long *et al.*, 1998] and permafrost bearing regions [Moskvitch, 2014]. This gives rise to perceptions that various aspects of methane release, utilization and related atmospheric chemistry changes await more research. For example, the magnitude of methane release from a collapsing cryosphere during the last 2.7 Ma and its climate amplifying potential remain of high interest considering projections for a future climate.

2 Summary of Articles

2.1 Article 1

Pavel Serov, Alexey Portnov, Jürgen Mienert, Petr Semenov, Polina Ilatovskaya (2015). **Methane release from pingo-like features across the South Kara Sea shelf, an area of thawing offshore permafrost.** *Journal of Geophysical Research: Earth Surface*. DOI: 10.1002/2015JF003467

During the last glacial maximum, 120 m sea-level drop emerged vast territories of a non-glaciated South Kara Sea shelf. Exposure to -15 °C mean annual air temperatures caused the formation of up to ~ 350 m thick permafrost. Subsequent transgression started ~19,000 years ago initiated thawing of the relic permafrost that is still ongoing today. Thawing permafrost may emit methane trapped inside frozen sediments in form of free gas and gas hydrate, as well as organic matter supporting microbial methanogenesis.

In **Article 1** we, for the first time, report and investigate ice-bearing domes (pingo-like features - PLF) on the West Yamal Shelf (40 – 80 m water depth) of the South Kara Sea. PLF 1 does not show any elevated methane concentrations on its surface and frozen sediments outcrop on the seafloor. PLF 2, in contrast, reveals evidence of thawing and elevated methane concentrations. In both locations, our geochemical results demonstrate a biogenic nature of methane gas and no contribution of heavier thermogenic hydrocarbons.

Combining our observations with published results of permafrost modeling we suggest a mechanism of permafrost-bound methane release involving decomposition of intra-permafrost gas hydrates. Further, we propose a range of possible scenarios of PLF formation in areas of subsea permafrost retreat and methane release that is important for many circum-Arctic regions.

Due to geothermal heat fluxes, subsea permafrost thaws from below despite cold (> -1 °C) bottom water temperatures on its upper boundary. The lower part of subsea permafrost is lying within the pressure / temperature field of methane hydrate phase stability. Retreat of the lower permafrost boundary causes a collapse of the associated GHSZ, hydrate-bound methane release, and pore pressure build up. Methane gas accumulating beneath progressively thinning permafrost may push-up the remaining permafrost cap forming a PLF. Higher methane concentration at PLF 2 may be explained by more pronounced thawing likely reflecting inhomogeneity in geothermal heat flux, initial ice saturation and lithological properties.

State of submarine and onshore permafrost in Yamal peninsula region has become concerning in light of recently occurred blow-out craters and our report of PLFs releasing methane. Yet scarce geophysical and drilling data limit our attempts to estimate current boundaries of permafrost, rate of its retreat and associated regional methane release.

2.2 Article 2

Pavel Serov, Sunil Vadakkepuliambatta, Jurgen Mienert, Henry Patton, Alexey Portnov, Anna Silyakova, Giuliana Panieri, Michael L. Carroll, JoLynn Carroll, Karin Andreassen, Alun Hubbard (2017). **Postglacial response of Arctic Ocean gas hydrates to climatic amelioration**. *Proceedings of the National Academy of Science of the United States of America (PNAS)*. DOI: 10.1073/pnas.1619288114

In **Article 2** we investigate the effect of environmental changes from the Last Glacial Maximum to the present day on the stability of gas hydrates on an Arctic Ocean continental margin. Our study integrates empirical observations of past and present seabed methane release in the previously glaciated Storfjorden trough in the north-western Barents Sea and a coupled ice-sheet/gas hydrate model to identify phases of subglacial methane sequestration and release.

Geophysical data reveal a group of seabed domes (350-500 m in diameter and 6-10 m high) at 370 – 390 m water depth bearing gas hydrates and releasing thermogenic hydrocarbon gas into the water column. The domes host abundant methane-derived authigenic carbonate formations visible on the seabed and appearing within a sediment section in distinct layers. Due to sufficient fraction of methane-derived carbonate formations and gas hydrates in soft cohesive sediments we refer the structures to gas hydrate pingos (GHPs). Layered appearance of methane-derived carbonate formations points toward variable intensity of seabed methane leakage in the past.

Our gas hydrate stability model is forced with transient subglacial pressure and temperature derived from ice-sheet model. The seafloor pressure and temperature is derived from existing sea-level curves and oxygen isotope records. The coupled model shows the dynamic nature of the GHSZ during the last 37,000 years. The onset of the glaciation provoked the build-up of GHSZ ~35,000 years BP. The 200-220 m thick glacially controlled GHSZ was present in Storfjorden Trough for 13,500 years until the retreat of the ice-sheet. Deglaciation caused depressurization and seabed warming due to removal of ice load and encroachment of ocean waters that reduced GHSZ to a c. 40 m thickness. Subsequently, the submarine GHSZ started to collapse due to ocean warming of bottom waters during Heinrich event H1 (15,000 – 13,000 years BP), the Bølling and Allerød interstadials (13,000 – 11,000 years BP) and the Holocene optimum (9,000 – 8,000 years BP). This triggered a release of hydrate-bound methane and migration of gas from deeper sources allowing more thermogenic gas to reach the seabed. The variability of methane efflux is documented in discrete appearances of methane-derived authigenic carbonates in post-glacial sediment sections.

Through synthesis of empirical data and hybrid ice-sheet/GHSZ modeling we show that an extensive gas hydrate system formed in subglacial conditions across Storfjorden Trough during the Last Glacial

Maximum. This system subsequently experienced repeated cycles of collapse and reemergence of gas hydrates due to changes in oceanographic conditions and glacio-isostatic adjustments. Our study shows that abrupt changes in pressure and temperature conditions related to interactions of grounded ice-sheets, postglacial isostatic rebound and influx of variable ocean currents modulate gas storage and release. Such study is deemed particularly important in the light of a potential collapse of the Greenland ice-sheet under future global warming.

2.3 Article 3

Karin Andreassen, Alun Hubbard, Monica Winsborrow, Henry Patton, Sunil Vadakkepuliambatta, Andreia Plaza-Faverola, Eythor Gudlaugsson, Pavel Serov, Alexey Deryabin, Rune Mattingdal, Jurgen Mienert, Stefan Bunz (2017). **Massive blow-out crater formed by hydrate-controlled methane expulsion from the Arctic seafloor.** *Science*. DOI: 10.1126/science.aal4500

A grounded ice-sheet controlled the evolution of a gas hydrate stability zone across the Barents Sea shelf. However, the magnitude of methane release due to postglacial gas hydrate decomposition remained elusive. In the **Article 3** we present geophysical data documenting >100 seabed methane-leaking craters up to 1.2 km wide and 35 m deep within 440 km² in previously glaciated Bjørnøya Trough. The craters are engraved in Middle-Triassic sedimentary bedrock covered with <2 m thick veneer of glacial deposits. 2D seismic data indicate a series of faults connecting Triassic hydrocarbon source and reservoir rocks documented at a strategic petroleum industry borehole to shallow gas accumulations.

Combining our observations of an extensive subsurface fluid flow system with a paired ice-sheet and GHSZ model we propose a conceptual scenario for the formation of craters in the northern Barents Sea. Cyclic episodes of Barents Sea ice-sheet loading and unloading throughout the Pleistocene caused perturbations of a subseabed pressure field in thermogenic gas reservoirs. This enhanced sub-vertical cracking and gas migration along faults into glacially-controlled GHSZ. Rapid retreat of grounded ice-sheet (17,000 – 15,000 years BP) caused a shoaling of lower GHSZ boundary, while a release of hydrate-bound methane contributed to hydrate growth in a still remaining but shallow and thin GHSZ. Volume increase due to hydrate growth and hydrofracturing led to GHP formation. Upon deglaciation, the seafloor overlain with a 320 m thick and warm water column was outside the GHSZ, leading to dissociation of hydrates within GHPs, followed by their collapse, methane expulsion and blow-out crater formation.

Thermogenic gas reservoirs affected by grounded ice-sheets are wide spread. A region of 33 million km² with confirmed hydrocarbon reserves offshore northern Europe, Russia, Canada and the United States was directly affected by the last glaciation [Ehlers and Gibbard, 2007]. Thus, analogous to our

study site, such glacially-controlled gas hydrate reservoirs may be common in many regions of the Arctic.

2.4 Article 4

Wei-Li Hong, Marta E. Torres, JoLynn Carroll, Antoine Cre´mie`re, Giuliana Panieri, Haoyi Yao, Pavel Serov (2017). **Seepage from an arctic shallow marine gas hydrate reservoir is insensitive to momentary ocean warming.** *Nature Communications*. DOI: 10.1038/ncomms15745

Gas hydrate accumulations located close to shallow termination of GHSZ across the Arctic Ocean continental margins are thought to have experienced gas hydrate dissociation induced by warming of ocean bottom water. In the **article 4** we investigate the potential influence of seasonal and decadal water temperature changes on gas hydrate pingos in Storfjorden Trough (380 m water depth).

Our geochemical analyses indicate concaved shapes of downcore profiles of (SO_4^{2-} , ΣHS , TA, Fe^{2+} , Ca^{2+} , Mg^{2+} and NH_4^+) in pore water pointing towards non-steady-state behavior of chemical species. Considering 5 potential reasons for such pattern, we model the responses of the pore water profiles to each of them. Our results show that increased methane flux is the most plausible candidate to explain observed non-steady-state geochemical profiles. Pore-water sulfate concentrations are used as proxy for anaerobic methane oxidation (AOM), which is controlled by upward flux of methane. The transport-reaction model of AOM indicates timing of enhanced methane ventilation events over different parts of one gas hydrate bearing mound (pingo). Further, we investigate if seasonal or decadal bottom warming trends may trigger gas hydrate dissociation and methane release. Considering seasonal temperature trends imposed on a longer-term trend of 1 °C warming of bottom water over 30 years we conclude that only 2.3 m of upper sediment section might experience gas hydrate dissociation that cannot explain methane flux matching with observed sulfate profiles.

Pre-anthropogenic age of methane flux events and limited contributions of recent bottom warming suggest that observed geochemical anomalies are not connected to ocean temperature-induced dissociation of gas hydrates. In turn, subseafloor controls of methane venting events such as pressure changes, opening and sealing of fractures are likely to explain increased methane fluxes in the past. These pulsations may be imposed on millennia-scale methane release events inferred from coupled ice-sheet/gas hydrate modeling (**Article 2**).

2.5 Article 5

Pavel Serov, Henry Patton, Malin Waage, Calvin Shackleton, Jürgen Mienert, Karin Andreassen. **Subglacial erosion and transportation of gas hydrate bearing sediments on an Arctic Ocean continental margin.** *Manuscript.*

Pleistocene glaciations of the Barents Sea shelf eroded up to 3 km of sedimentary strata. In areas where methane fluxes are sufficient to support gas hydrate formation, glacial erosion may affect subglacial gas hydrate inventories previously considered undisturbed under the thick ice. In the **Article 5** we investigate the erosion effect of LGM Storfjordrenna Ice Stream on gas hydrate bearing deposits in an area of strong thermogenic gas leakage from a deep source.

Here we use 1 dimensional multiphase fluid flow and gas hydrate model TOUGH+ HYDRATE [Moridis, 2014] to simulate evolution of gas hydrate, free and dissolved gas in pore space of deposits underlying the LGM Storfjordrenna ice stream. The model is constrained with empirical data revealing sediment thicknesses, stratigraphy, and active subseabed migration of thermogenic gas. Analogous to **Article 2**, we force our gas hydrate model with ice thickness, bottom temperature and isostatically adjusting topography derived from the UiT ice-sheet model. Moreover, we introduce transient seabed erosion parameter acquired through adjusting previously published average erosion rates with varying basal velocity of the ice stream. We assume that higher velocities of the Storfjordrenna Ice Stream at ice - sediment interface correspond to higher rates of subglacial erosion. In order to show a range of possible scenarios we consider 3 different average erosion rates consistent with literature: 1.0 mm/yr, 1.7 mm/yr – the most likely scenario, and 3.0 mm/yr.

The modeling indicates that, depending on the average erosion rate scenario, 13.4 – 40.2 m of sediments is eroded during ~14,100 years interval of ice-sheet dominating our study area. These sediment erosion values correspond to 0.11 – 0.32 m³ of methane hydrate eroded from 1 m² of seafloor at areas of active methane release during the LGM. These values are comparable to amount of hydrate that are predicted to disappear from 1 m² of western Svalbard shelf at 400 m water depth by the end of the 21st Century [Marín-Moreno *et al.*, 2015].

Extrapolating our point estimates, within 5 gas migration conduits (total area 137,500 m²) mapped at the study area using high-resolution P-cable 3D seismic technology the LGM glacial erosion may remove 15,125 to 44,000 m³ of methane hydrate. Eroded hydrate-bearing deposits may be frozen into the ice or dissolved in subglacial water and transported to the ice margin. It is very likely that some portions of glacially eroded methane hydrate or dissolved hydrate-bound gas reach the ice margin and discharge into the ocean during glaciations. Taking into account wide availability of methane sources and fluid leakage structures across the Barents Sea shelf experienced > 30 glacial cycles, the

implications of subglacial denudation of gas hydrate-bearing sediments for ocean methane uptake may be much broader.

3 Future research

First attempts to investigate the behavior of the cryosphere-dependent methane inventories throughout the last glacial cycle showed a potential significance of expanding similar multidisciplinary studies to earlier glaciations and to the future scenarios of the Greenland ice-sheet dynamics. Since 2.7 ma, the Barents Sea shelf experienced up to 30 cycles of glaciation – deglaciation [Knies *et al.*, 2009], some of which might also have impacted the South Kara Sea shelf. Limited amount of empirical constrains on ice-sheet evolution and paleo fluid flow is a major challenge. However, despite late Weichselian glaciation “reset” seabed imprints and underlying geological features of previous glacial cycles, trough mouth fans and some shelf areas may still preserve valuable stratigraphic records of older glacial cycles. Relying on these empirical constrains, CAGE is developing a model of Pleistocene evolution of the Barents Sea Ice-sheet that would be of great importance for reconstructing gas hydrate dynamics and seabed methane release history. Here, the dynamics of the Greenland ice-sheet and its impacts on gas reservoirs is today’s best analogue in a rapidly changing world during climate change [Hanna *et al.*, 2013; Robinson *et al.*, 2012]. Greenland with the large shelf areas could be one of the key regions for observing environmental changes on the seabed.

Investigating glacial/interglacial deposits of Pleistocene glacial cycles for potential fluid flow features using high-resolution 3D seismic P-Cable surveys may provide new insights into paleo methane release dynamics connecting numerical modeling with actual geological observations. Stratigraphic correlation of glacial units bearing fluid flow features would provide tentative age constrains of fluid migration patterns. Drilling campaigns concentrating on methane-derived authigenic carbonate records may further contribute to verify age of methane release events.

Another direction of potential future research comes with in situ measurements of methane concentrations and studies of methane oxidizing biomass in front of active marine terminating ice streams of Greenland. It may shed more light on similar scenarios of the former environmental conditions along the western Barents Sea ice-sheet. The conceptual scenarios of subglacial methane sequestration and postglacial release that we proposed in Articles 2, 3 and 5 neglect potential bacterial utilization of methane. Very limited amount of literature on subglacial methane microbiology, as well as in situ measurements of methane concentrations in front of marine terminated ice-sheets exists today. Understanding of methane turnover in subglacial environments is important for assessing feedbacks and climate accelerators in a changing Arctic under future warming.

List of figures

Figure 1 – Release of methane gas and surrounding pavements of authigenic carbonates offshore Virginia, Atlantic Ocean. Image by NOAA Okeanos Explorer program, 2013 Northeast U.S. Expedition. Public domain

Figure 2 – Gas hydrate pingos (M1 – M8) on shaded relief map (A) and bathymetric map (B) in the Kwanza Basin, offshore Angola [Serié *et al.*, 2012]

Figure 3 - Blowout at 22/4b well in the North Sea, November 1990 (modified after Leifer and Judd [2015] and Schneider von Deimling *et al.* [2015]). a - surface expression of a gas plume. Insert shows gas bubbles observed on the sea surface at 22/4b site during a research cruise in 2005 [Leifer and Judd, 2015]; b – gridded multibeam bathymetry data and a topographic profile showing 20 m deep crater formed at the site [Schneider von Deimling *et al.*, 2015]

Figure 4 – Maximum ice-sheet extent of the Barents Sea and Fennoscandian Ice-sheets and their major drainage pathways [Patton *et al.*, 2017]

Figure 5 – seabed topography change due to isostatic rebound of the Barents Sea shelf [Patton *et al.*, 2017].

Figure 6 – Global sea-level predictions (lines) and relative sea-level data (dots) for New Guinea (light blue) and Barbados (dark blue). Grey line indicates eustatic sea-level time series [Clark *et al.*, 2009]

Figure 7 – Location of the study areas in relation to limits of the LGM Barents Sea Ice-sheet, 120m isobath marking the maximum seaward limit of relic subsea permafrost, and 390m isobaths indicating tentative shallow termination of methane hydrate stability zone [Jakobsson *et al.*, 2012]

Figure 8 – (a) Eustatic sea level curves defining exposure time of the Yamal Shelf [Fleming *et al.*, 1998; Lea *et al.*, 2003]. (b) Modeled extent of permafrost during the LGM sea level lowstand (light blue) and today (dark blue) [Portnov *et al.*, 2014]

Figure 9 – Hydro-acoustic anomalies on Yamal shelf (yellow lines) concentrating in water depth deeper than 20 m (shown in blue). Black lines show locations of survey lines [Portnov *et al.*, 2013]

Figure 10 - Seabed topography of the western Barents Sea margin with location of study areas 3 in Storfjorden trough and study area 4 in Bjørnøya trough [Jakobsson *et al.*, 2012]

Figure 11 – δD H₂O, methane, $\delta^{13}CH_4$ and carbon dioxide records [Moller *et al.*, 2013]. Ice cores from Vostok, EDML, Talos Dome, Byrd, EPICA Dome C and GISP2 are used for composed curves

Figure 12 – Observed global temperature changes and modeled future climatic feedback in response to variable anthropogenic CO₂ emission scenarios (IPCC special report on Global warming of 1.5 °C)

Figure 13 - Sources and sinks of hydrate-bound methane [Ruppel and Kessler, 2017]

Reference

- Alley, R. B. (2000), Ice-core evidence of abrupt climate changes, *Proceedings of the National Academy of Sciences*, 97(4), 1331-1334, doi:10.1073/pnas.97.4.1331.
- Alley, R. B., and P. U. Clark (1999), THE DEGLACIATION OF THE NORTHERN HEMISPHERE: A Global Perspective, *Annual Review of Earth and Planetary Sciences*, 27(1), 149-182, doi:10.1146/annurev.earth.27.1.149.
- Andreassen, K., et al. (2017), Massive blow-out craters formed by hydrate-controlled methane expulsion from the Arctic seafloor, *Science*, 356(6341), 948-953, doi:10.1126/science.aal4500.
- Anell, I. M., J. I. Faleide, and A. Braathen (2016), Regional tectono-sedimentary development of the highs and basins of the northwestern Barents Shelf, *Norsk Geologisk Tidsskrift*, 96(1), 27-41.
- Archer, D. (2015), A model of the methane cycle, permafrost, and hydrology of the Siberian continental margin, *Biogeosciences*, 12(10), 2953-2974.
- Auriac, A., P. L. Whitehouse, M. J. Bentley, H. Patton, J. M. Lloyd, and A. Hubbard (2016), Glacial isostatic adjustment associated with the Barents Sea ice-sheet: A modelling inter-comparison, *Quaternary Science Reviews*, 147, 122-135, doi:<http://dx.doi.org/10.1016/j.quascirev.2016.02.011>.
- Bergh, S. G., and P. Grogan (2003), Tertiary structure of the Sørkapp-Hornsund Region, South Spitsbergen, and implications for the offshore southern extension of the fold-thrust Belt, *Norwegian Journal of Geology*, 83, 43-60.
- Boetius, A., K. Ravenschlag, C. J. Schubert, D. Rickert, F. Widdel, A. Gieseke, R. Amann, B. B. Jorgensen, U. Witte, and O. Pfannkuche (2000), A marine microbial consortium apparently mediating anaerobic oxidation of methane, *Nature*, 407(6804), 623-626, doi:http://www.nature.com/nature/journal/v407/n6804/supinfo/407623a0_S1.html.
- Brook, E. J. (2005), Tiny Bubbles Tell All, *Science*, 310(5752), 1285-1287, doi:10.1126/science.1121535.
- Bröder, L., T. Tesi, A. Andersson, I. Semiletov, and Ö. Gustafsson (2018), Bounding cross-shelf transport time and degradation in Siberian-Arctic land-ocean carbon transfer, *Nature Communications*, 9(1), 806, doi:10.1038/s41467-018-03192-1.
- Callaghan, T. V., M. Johansson, J. Key, T. Prowse, M. Ananicheva, and A. Klepikov (2011), Feedbacks and Interactions: From the Arctic Cryosphere to the Climate System, *Ambio*, 40(Suppl 1), 75-86, doi:10.1007/s13280-011-0215-8.
- Chappellaz, J., et al. (2013), High-resolution glacial and deglacial record of atmospheric methane by continuous-flow and laser spectrometer analysis along the NEEM ice core, *Climate of the Past*, 9, 2579-2593, doi:10.5194/cp-9-2579-2013.
- Clark, P. U., A. S. Dyke, J. D. Shakun, A. E. Carlson, J. Clark, B. Wohlfarth, J. X. Mitrovica, S. W. Hostetler, and A. M. McCabe (2009), The Last Glacial Maximum, *Science*, 325(5941), 710-714, doi:10.1126/science.1172873.
- Cranston, R. (1994), Marine sediments as a source of atmospheric methane, *Bulletin of the Geological Society of Denmark*, 41, 101-109.

- Cremiere, A., A. Lepland, S. Chand, D. Sahy, D. J. Condon, S. R. Noble, T. Martma, T. Thorsnes, S. Sauer, and H. Brunstad (2016), Timescales of methane seepage on the Norwegian margin following collapse of the Scandinavian Ice-sheet, *Nat Commun*, 7, doi:10.1038/ncomms11509.
- Dickens, G. R., C. K. Paull, and P. Wallace (1997), Direct measurement of in situ methane quantities in a large gas-hydrate reservoir, *Nature*, 385, 426, doi:10.1038/385426a0.
- Du, M., and J. D. Kessler (2012), Assessment of the Spatial and Temporal Variability of Bulk Hydrocarbon Respiration Following the Deepwater Horizon Oil Spill, *Environmental Science & Technology*, 46(19), 10499-10507, doi:10.1021/es301363k.
- Ehlers, J., and P. L. Gibbard (2007), The extent and chronology of Cenozoic global glaciation, *Quaternary International*, 164, 6-20.
- Fleming, K., P. Johnston, D. Zwartz, Y. Yokoyama, K. Lambeck, and J. Chappell (1998), Refining the eustatic sea-level curve since the Last Glacial Maximum using far- and intermediate-field sites, *Earth and Planetary Science Letters*, 163(1), 327-342, doi:[https://doi.org/10.1016/S0012-821X\(98\)00198-8](https://doi.org/10.1016/S0012-821X(98)00198-8).
- Gautier, D. L., et al. (2009), Assessment of Undiscovered Oil and Gas in the Arctic, *Science*, 324(5931), 1175-1179, doi:10.1126/science.1169467.
- Ginsburg, G. (1998), Gas hydrate accumulation in deep-water marine sediments, *Geological Society, London, Special Publications*, 137(1), 51-62.
- Grama, Y. (2012), The analysis of Russian oil and gas reserves, *International Journal of Energy Economics and Policy*, 2(2), 82-91.
- Graves, C. A., L. Steinle, G. Rehder, H. Niemann, D. P. Connelly, D. Lowry, R. E. Fisher, A. W. Stott, H. Sahling, and R. H. James (2015), Fluxes and fate of dissolved methane released at the seafloor at the landward limit of the gas hydrate stability zone offshore western Svalbard, *Journal of Geophysical Research: Oceans*, 120(9), 6185-6201, doi:10.1002/2015JC011084.
- Greinert, J., Y. Artemov, V. Egorov, M. De Batist, and D. McGinnis (2006), 1300-m-high rising bubbles from mud volcanoes at 2080 m in the Black Sea: Hydroacoustic characteristics and temporal variability, *Earth and Planetary Science Letters*, 244(1-2), 1-15, doi:<http://dx.doi.org/10.1016/j.epsl.2006.02.011>.
- Hanna, E., P. Huybrechts, K. Steffen, J. Cappelen, R. Huff, C. Shuman, T. Irvine-Fynn, S. Wise, and M. Griffiths (2008), Increased runoff from melt from the Greenland Ice-sheet: a response to global warming, *Journal of Climate*, 21(2), 331-341.
- Hanna, E., et al. (2013), Ice-sheet mass balance and climate change, *Nature*, 498, 51, doi:10.1038/nature12238.
- Harris, C., and J. B. Murton (2005), Cryospheric systems: glaciers and permafrost, Geological Society of London.
- Hill, T. M., J. P. Kennett, D. L. Valentine, Z. Yang, C. M. Reddy, R. K. Nelson, R. J. Behl, C. Robert, and L. Beaufort (2006), Climatically driven emissions of hydrocarbons from marine sediments during deglaciation, *Proceedings of the National Academy of Sciences*, 103(37), 13570-13574, doi:10.1073/pnas.0601304103.
- Høy, T., and B. Lundschieen (2011), Triassic deltaic sequences in the northern Barents Sea, *Geological Society, London, Memoirs*, 35(1), 249-260.
- Inagaki, F., et al. (2006), Biogeographical distribution and diversity of microbes in methane hydrate-bearing deep marine sediments on the Pacific Ocean Margin, *Proceedings of the National Academy of Sciences of the United States of America*, 103(8), 2815-2820, doi:10.1073/pnas.0511033103.
- Jakobsson, M., et al. (2014), Arctic Ocean glacial history, *Quaternary Science Reviews*, 92, 40-67, doi:<http://dx.doi.org/10.1016/j.quascirev.2013.07.033>.

- Jakobsson, M., et al. (2012), The International Bathymetric Chart of the Arctic Ocean (IBCAO) Version 3.0, *Geophysical Research Letters*, 39(12), n/a-n/a, doi:10.1029/2012GL052219.
- James, R. H., et al. (2016), Effects of climate change on methane emissions from seafloor sediments in the Arctic Ocean: A review, *Limnology and Oceanography*, n/a-n/a, doi:10.1002/lno.10307.
- Judd, A., and M. Hovland (2009), Seabed fluid flow: the impact on geology, biology and the marine environment, edited, Cambridge University Press.
- Kizyakov, A., M. Zimin, A. Sonyushkin, Y. Dvornikov, A. Khomutov, and M. Leibman (2017), Comparison of Gas Emission Crater Geomorphodynamics on Yamal and Gydan Peninsulas (Russia), Based on Repeat Very-High-Resolution Stereopairs, *Remote Sensing*, 9(10), 1023.
- Knies, J., J. Matthiessen, C. Vogt, J. S. Laberg, B. O. Hjelstuen, M. Smelror, E. Larsen, K. Andreassen, T. Eidvin, and T. O. Vorren (2009), The Plio-Pleistocene glaciation of the Barents Sea–Svalbard region: a new model based on revised chronostratigraphy, *Quaternary Science Reviews*, 28(9–10), 812-829, doi:<http://dx.doi.org/10.1016/j.quascirev.2008.12.002>.
- Koch, S., C. Berndt, J. Bialas, M. Haeckel, G. Crutchley, C. Papenberg, D. Klaeschen, and J. Greinert (2015), Gas-controlled seafloor doming, *Geology*, doi:10.1130/g36596.1.
- Laberg, Andreassen, and Vorren (2012), Late Cenozoic erosion of the high-latitude southwestern Barents Sea shelf revisited, *Geological Society of America Bulletin*, 124(1-2), 77-88.
- Lasabuda, A., J. S. Laberg, S.-M. Knutsen, and P. Safronova (2018), Cenozoic tectonostratigraphy and pre-glacial erosion: A mass-balance study of the northwestern Barents Sea margin, Norwegian Arctic, *Journal of Geodynamics*, doi:<https://doi.org/10.1016/j.jog.2018.03.004>.
- Lea, D., P. Martin, D. Pak, and H. Spero (2003), 350 kyr sea level reconstruction and foraminifer isotope data, IGBP PAGES/World Data Center A for Paleoclimatology Data Contribution Series# 2003-010, NOAA/NGDC.(Paleoclimatology Program, Boulder.
- Leifer, I., and A. Judd (2015), The UK22/4b blowout 20 years on: Investigations of continuing methane emissions from subseabed to the atmosphere in a North Sea context, *Marine and Petroleum Geology*, 68, 706-717, doi:<http://dx.doi.org/10.1016/j.marpetgeo.2015.11.012>.
- Leifer, I., B. P. Luyendyk, J. Boles, and J. F. Clark (2006), Natural marine seepage blowout: Contribution to atmospheric methane, *Global Biogeochemical Cycles*, 20(3), n/a-n/a, doi:10.1029/2005GB002668.
- Levin, L. A., et al. (2016), Hydrothermal Vents and Methane Seeps: Rethinking the Sphere of Influence, *Frontiers in Marine Science*, 3(72), doi:10.3389/fmars.2016.00072.
- Long, D., S. Lammers, and P. Linke (1998), Possible hydrate mounds within large sea-floor craters in the Barents Sea, *Geological Society, London, Special Publications*, 137(1), 223-237, doi:10.1144/gsl.sp.1998.137.01.18.
- Lundschien, B. A., T. Høy, and A. Mørk (2014), Triassic hydrocarbon potential in the Northern Barents Sea; integrating Svalbard and stratigraphic core data, *Norwegian Petroleum Directorate Bulletin*, 11, 3-20.
- Marín-Moreno, H., T. A. Minshull, G. K. Westbrook, and B. Sinha (2015), Estimates of future warming-induced methane emissions from hydrate offshore west Svalbard for a range of climate models, *Geochemistry, Geophysics, Geosystems*, 16(5), 1307-1323, doi:10.1002/2015GC005737.
- Mau, S., J. Blees, E. Helmke, H. Niemann, and E. Damm (2013), Vertical distribution of methane oxidation and methanotrophic response to elevated methane concentrations in stratified waters of the Arctic fjord Storfjorden (Svalbard, Norway), *Biogeosciences*, 10(10), 6267-6278, doi:10.5194/bg-10-6267-2013.
- Mau, S., et al. (2017), Widespread methane seepage along the continental margin off Svalbard - from Bjørnøya to Kongsfjorden, *Scientific Reports*, 7, 42997, doi:10.1038/srep42997

- Mix, A. C., E. Bard, and R. Schneider (2001), Environmental processes of the ice age: land, oceans, glaciers (EPILOG), *Quaternary Science Reviews*, 20(4), 627-657, doi:[https://doi.org/10.1016/S0277-3791\(00\)00145-1](https://doi.org/10.1016/S0277-3791(00)00145-1).
- Moller, L., T. Sowers, M. Bock, R. Spahni, M. Behrens, J. Schmitt, H. Miller, and H. Fischer (2013), Independent variations of CH₄ emissions and isotopic composition over the past 160,000 years, *Nature Geosci*, 6(10), 885-890, doi:10.1038/ngeo1922
- Moridis, G. J. (2014), TOUGH+ HYDRATE v1. 2 User's Manual: A Code for the Simulation of System Behavior in Hydrate-Bearing Geologic Media.
- Moskvitch, K. (2014), Mysterious Siberian crater attributed to methane, in *nature news*, edited, nature publishing group, doi:doi:10.1038/nature.2014.15649.
- Myhre, C. L., et al. (2016), Extensive release of methane from Arctic seabed west of Svalbard during summer 2014 does not influence the atmosphere, *Geophysical Research Letters*, 43(9), 4624-4631, doi:10.1002/2016GL068999.
- Nelson, F. E., O. A. Anisimov, and N. I. Shiklomanov (2001), Subsidence risk from thawing permafrost, *Nature*, 410, 889, doi:10.1038/35073746.
- Pachauri, R. K., M. R. Allen, V. R. Barros, J. Broome, W. Cramer, R. Christ, J. A. Church, L. Clarke, Q. Dahe, and P. Dasgupta (2014), *Climate change 2014: synthesis report. Contribution of Working Groups I, II and III to the fifth assessment report of the Intergovernmental Panel on Climate Change*, IPCC.
- Parkinson, C. L., and D. J. Cavalieri (2008), Arctic sea ice variability and trends, 1979–2006, *Journal of Geophysical Research: Oceans*, 113(C7).
- Patton, K. Andreassen, L. R. Bjarnadóttir, J. A. Dowdeswell, M. C. M. Winsborrow, R. Noormets, L. Polyak, A. Auriac, and A. Hubbard (2015), Geophysical constraints on the dynamics and retreat of the Barents Sea ice-sheet as a paleobenchmark for models of marine ice-sheet deglaciation, *Reviews of Geophysics*, 53(4), 1051-1098, doi:10.1002/2015RG000495.
- Patton, Hubbard, Andreassen, Auriac, P. L. Whitehouse, A. P. Stroeven, C. Shackleton, M. Winsborrow, J. Heyman, and A. M. Hall (2017), Deglaciation of the Eurasian ice-sheet complex, *Quaternary Science Reviews*, 169, 148-172, doi:<http://dx.doi.org/10.1016/j.quascirev.2017.05.019>.
- Patton, Hubbard, Andreassen, Winsborrow, and A. P. Stroeven (2016), The build-up, configuration, and dynamical sensitivity of the Eurasian ice-sheet complex to Late Weichselian climatic and oceanic forcing, *Quaternary Science Reviews*, 153, 97-121, doi:<http://dx.doi.org/10.1016/j.quascirev.2016.10.009>.
- Paull, C. K., W. Ussler, S. R. Dallimore, S. M. Blasco, T. D. Lorenson, H. Melling, B. E. Medioli, F. M. Nixon, and F. A. McLaughlin (2007), Origin of pingo-like features on the Beaufort Sea shelf and their possible relationship to decomposing methane gas hydrates, *Geophysical Research Letters*, 34(1), n/a-n/a, doi:10.1029/2006GL027977.
- Platt, S. M., S. Eckhardt, B. Ferré, R. E. Fisher, O. Hermansen, P. Jansson, D. Lowry, E. G. Nisbet, I. Pisso, and N. Schmidbauer (2018), Methane at Svalbard and over the European Arctic Ocean.
- Pohlman, J. W., J. Greinert, C. Ruppel, A. Silyakova, L. Vielstädte, M. Casso, J. Mienert, and S. Bünz (2017), Enhanced CO₂ uptake at a shallow Arctic Ocean seep field overwhelms the positive warming potential of emitted methane, *Proceedings of the National Academy of Sciences*, doi:10.1073/pnas.1618926114.
- Portnov, A., J. Mienert, and P. Serov (2014), Modeling the evolution of climate-sensitive Arctic subsea permafrost in regions of extensive gas expulsion at the West Yamal shelf, *Journal of Geophysical Research: Biogeosciences*, 119(11), 2082-2094, doi:10.1002/2014JG002685.

- Portnov, A., J. Mienert, M. Winsborrow, K. Andreassen, S. Vadakkepuliambatta, P. Semenov, and V. Gataullin (2018), Shallow carbon storage in ancient buried thermokarst in the South Kara Sea, *Scientific Reports*, 8(1), 14342, doi:10.1038/s41598-018-32826-z.
- Portnov, A., A. J. Smith, J. Mienert, G. Cherkashov, P. Rekant, P. Semenov, P. Serov, and B. Vanshtein (2013), Offshore permafrost decay and massive seabed methane escape in water depths >20 m at the South Kara Sea shelf, *Geophysical Research Letters*, 40(15), 3962-3967, doi:doi:10.1002/grl.50735.
- Portnov, A., S. Vadakkepuliambatta, J. Mienert, and A. Hubbard (2016), Ice-sheet-driven methane storage and release in the Arctic, *Nat Commun*, 7, doi:10.1038/ncomms10314.
- Rasmussen, T. L., E. Thomsen, M. A. Ślubowska, S. Jessen, A. Solheim, and N. Koç (2007), Paleoceanographic evolution of the SW Svalbard margin (76°N) since 20,000 14C yr BP, *Quaternary Research*, 67(1), 100-114, doi:<http://dx.doi.org/10.1016/j.yqres.2006.07.002>.
- Reeburgh, W. S. (2007), Oceanic Methane Biogeochemistry, *Chemical Reviews*, 107(2), 486-513, doi:10.1021/cr050362v.
- Rekant, P., and A. Vasiliev (2011), Distribution of subsea permafrost at the Kara Sea shelf, *Cryosphere of the Earth*, XV, 4, 69-72.
- Rhee, T. S., A. J. Kettle, and M. O. Andreae (2009), Methane and nitrous oxide emissions from the ocean: A reassessment using basin-wide observations in the Atlantic, *Journal of Geophysical Research: Atmospheres*, 114(D12), n/a-n/a, doi:10.1029/2008JD011662.
- Rignot, E., and R. H. Thomas (2002), Mass Balance of Polar Ice-sheets, *Science*, 297(5586), 1502-1506, doi:10.1126/science.1073888.
- Robinson, A., R. Calov, and A. Ganopolski (2012), Multistability and critical thresholds of the Greenland ice-sheet, *Nature Climate Change*, 2, 429, doi:10.1038/nclimate1449
- Ruff, S. E., J. F. Biddle, A. P. Teske, K. Knittel, A. Boetius, and A. Ramette (2015), Global dispersion and local diversification of the methane seep microbiome, *Proceedings of the National Academy of Sciences*, 112(13), 4015-4020, doi:10.1073/pnas.1421865112.
- Ruppel, C. D., and J. D. Kessler (2017), The interaction of climate change and methane hydrates, *Reviews of Geophysics*, n/a-n/a, doi:10.1002/2016RG000534.
- Sahling, H., et al. (2014), Gas emissions at the continental margin west of Svalbard: mapping, sampling, and quantification, *Biogeosciences*, 11(21), 6029-6046, doi:10.5194/bg-11-6029-2014.
- Sazonova, T. S., V. E. Romanovsky, J. E. Walsh, and D. O. Sergueev (2004), Permafrost dynamics in the 20th and 21st centuries along the East Siberian transect, *Journal of Geophysical Research: Atmospheres*, 109(D1), doi:doi:10.1029/2003JD003680.
- Schneider von Deimling, J., P. Linke, M. Schmidt, and G. Rehder (2015), Ongoing methane discharge at well site 22/4b (North Sea) and discovery of a spiral vortex bubble plume motion, *Marine and Petroleum Geology*, 68, Part B, 718-730, doi:<https://doi.org/10.1016/j.marpetgeo.2015.07.026>.
- Serié, C., M. Huuse, and N. H. Schødt (2012), Gas hydrate pingoes: Deep seafloor evidence of focused fluid flow on continental margins, *Geology*, 40(3), 207-210, doi:10.1130/G32690.1.
- Sévellec, F., A. V. Fedorov, and W. Liu (2017), Arctic sea-ice decline weakens the Atlantic Meridional Overturning Circulation, *Nature Climate Change*, 7, 604, doi:10.1038/nclimate3353
- Shakhova, N., I. Semiletov, I. Leifer, A. Salyuk, P. Rekant, and D. Kosmach (2010), Geochemical and geophysical evidence of methane release over the East Siberian Arctic Shelf, *Journal of Geophysical Research: Oceans*, 115(C8), n/a-n/a, doi:10.1029/2009JC005602.

- Shakhova, N., et al. (2015), The East Siberian Arctic Shelf: towards further assessment of permafrost-related methane fluxes and role of sea ice, *Philosophical Transactions of the Royal Society of London A: Mathematical, Physical and Engineering Sciences*, 373(2052), doi:10.1098/rsta.2014.0451.
- Siegert, M. J., J. A. Dowdeswell, M. Hald, and J.-I. Svendsen (2001), Modelling the Eurasian Ice-sheet through a full (Weichselian) glacial cycle, *Global and Planetary Change*, 31(1), 367-385, doi:[http://dx.doi.org/10.1016/S0921-8181\(01\)00130-8](http://dx.doi.org/10.1016/S0921-8181(01)00130-8)
- Slaymaker, O., and R. Kelly (2009), *The cryosphere and global environmental change*, John Wiley & Sons.
- Sloan, E. D., C. Koh (2008), *Clathrate Hydrates of Natural Gases*, 3rd ed., CRC Press, Boca Raton, Fla.
- Sowers, T. (2006), Late Quaternary Atmospheric CH₄ Isotope Record Suggests Marine Clathrates Are Stable, *Science*, 311(5762), 838-840, doi:10.1126/science.1121235.
- Steinle, L., et al. (2015), Water column methanotrophy controlled by a rapid oceanographic switch, *Nature Geosci*, 8(5), 378-382, doi:10.1038/ngeo2420
- Stocker, T. (2014), *Climate change 2013: the physical science basis: Working Group I contribution to the Fifth assessment report of the Intergovernmental Panel on Climate Change*, Cambridge University Press.
- Stupakova, A. (2011), Structure and petroleum potential of the Barents-Kara Shelf and adjacent territories, *Oil and gas geology*, 6(6), 99-115.
- Sultan, N., et al. (2004), Triggering mechanisms of slope instability processes and sediment failures on continental margins: a geotechnical approach, *Marine Geology*, 213(1), 291-321, doi:<https://doi.org/10.1016/j.margeo.2004.10.011>.
- Vadakkepuliyambatta, S., S. Chand, and S. Bünz (2017), The history and future trends of ocean warming-induced gas hydrate dissociation in the SW Barents Sea, *Geophysical Research Letters*, 44(2), 835-844, doi:doi:10.1002/2016GL071841.
- Wadham, J. L., et al. (2012), Potential methane reservoirs beneath Antarctica, *Nature*, 488(7413), 633-637, doi:<http://www.nature.com/nature/journal/v488/n7413/abs/nature11374.html#supplementary-information>.
- Wadham, J. L., M. Tranter, S. Tulaczyk, and M. Sharp (2008), Subglacial methanogenesis: A potential climatic amplifier?, *Global Biogeochemical Cycles*, 22(2), n/a-n/a, doi:10.1029/2007GB002951.
- Wallmann, K., et al. (2018), Gas hydrate dissociation off Svalbard induced by isostatic rebound rather than global warming, *Nature Communications*, 9(1), 83, doi:10.1038/s41467-017-02550-9.
- Winsborrow, M. C. M., K. Andreassen, G. D. Corner, and J. S. Laberg (2010), Deglaciation of a marine-based ice-sheet: Late Weichselian palaeo-ice dynamics and retreat in the southern Barents Sea reconstructed from onshore and offshore glacial geomorphology, *Quaternary Science Reviews*, 29(3), 424-442, doi:<https://doi.org/10.1016/j.quascirev.2009.10.001>.
- Yakushev, V. S., and E. M. Chuvilin (2000), Natural gas and gas hydrate accumulations within permafrost in Russia, *Cold Regions Science and Technology*, 31(3), 189-197, doi:[https://doi.org/10.1016/S0165-232X\(00\)00012-4](https://doi.org/10.1016/S0165-232X(00)00012-4).
- Åström, E. K. L., M. L. Carroll, W. G. Ambrose, A. Sen, A. Silyakova, and J. Carroll (2018), Methane cold seeps as biological oases in the high-Arctic deep sea, *Limnology and Oceanography*, 63(S1), S209-S231, doi:doi:10.1002/lno.10732.

Article 1

Pavel Serov, Alexey Portnov, Jürgen Mienert, Petr Semenov, Polina Ilatovskaya (2015).

Methane release from pingo-like features across the South Kara Sea shelf, an area of thawing offshore permafrost. *Journal of Geophysical Research: Earth Surface*. DOI: 10.1002/2015JF003467